

Table 6 The summary of non-CJD patients in the positive cases of ELISA of 14-3-3 γ protein

Age	Sex	diagnosis	WB (14-3-3 protein)		ELISA	Real-time QUIC method
			all isoforms	γ -specific isoform	γ -specific isoform	
79	male	PCD/LEMS	+	+	4, 233	-
69	male	PCD/LEMS	+	+	4, 541	-
51	female	temporal epilepsy	+	+	3, 405	-
59	female	temporal epilepsy	+	+	3, 796	-
62	male	limbic encephalitis	+	+	3, 072	-
78	male	limbic encephalitis	+	+	5, 809	-
42	female	MELAS	+	+	4, 912	-
25	female	MELAS	+	+	5, 227	-
78	male	DAT	+	+	3, 110	-
62	female	DAT	+	+	3, 386	-
69	female	DAT	+	+	3, 892	-
57	male	DAT	+	-	3, 092	-
59	male	DAT	+	-	3, 074	-
61	male	DAT	+	-	3, 038	-
66	female	DAT	+	-	2, 941	-
67	female	DAT	-	-	2, 569	-
70	female	DAT	-	-	2, 534	-
78	female	DAT	-	-	2, 445	-
83	female	DAT	-	-	2, 410	-
89	female	DAT	-	-	2, 025	-
72	male	DAT	-	-	1, 949	-
59	female	DAT	-	-	1, 852	-
63	male	DAT	-	-	1, 709	-

PCD: paraneoplastic cerebellar degeneration, LEMS: Lambert-Eaton myasthenic syndrome, MELAS: Mitochondrial myopathy, Encephalopathy, Lactic Acidosis, Stroke-like episodes, DAT: Dementia of Alzheimer's type

found that all three protein markers in CSF to be highly sensitive at the early stages of CJD, with CSF tau protein having the greatest specificity and efficiency. However, an ELISA to detect 14-3-3 was the most sensitive of the biochemical markers from the same samples. These findings indicate that a combination of DWI-MRI and 14-3-3 γ ELISA are the most effective tests for detecting CSF protein markers during the early stages of CJD.

There were two problems with our study: 20 DAT cases identified that the level of ELISA was 3, 000-5, 000 AU/ml, but they could not be detected by WB and these results showed a discrepancy between the 14-3-3 γ WB and ELISA (additional file 3, figure S1-a); and the specificity of the ELISA was very low (Figure 1). In this study we established an ELISA method for the detection of 14-3-3 γ in CSF. The levels of 14-3-3 in the CSF of CJD patients were significantly elevated compared with those in other patients with neurological disorders. In various studies, the differences in sensitivity and specificity for detection of 14-3-3 were likely due to the lack of uniformity between the diseases, as well as the number of diseases that are associated with 14-3-3. The detection limit of the γ -isoform by WB was equivalent to 3, 400-4, 600 AU/ml by the ELISA, thus very low

levels of 14-3-3 γ in the CSF of DAT patients were confirmed using the ELISA (Table 6).

One of the reasons why the specificity was low was the combination of monoclonal antibodies used in the sandwich ELISA. If we had developed the ELISA using a combination of specific γ -isoform antibodies, such as clone #3, it is likely that the specificity may have been greater.

Atarashi et al. [7] detected the abnormal prion protein in CSF using the RT-QUIC method, with the specificity of the RT-QUIC method at 100%. These findings indicate the promise of an enhanced diagnostic capacity of RT-QUIC in the antemortem evaluation of suspected CJD. The RT-QUIC method has high specificity and moderate sensitivity in suspected CJD cases. Therefore, the cut-off limit for ELISA assay sensitivity was close to 100% because the specificity of the RT-QUIC method was 100%. Differential diagnosis is crucial, in particular because the number of false positive results may increase (Table 6). Additionally, the subtype of false negative results with human prion disease is also important (Tables 4 and 5).

Conclusion

We have established an ELISA that specifically detects 14-3-3 γ , and we believe that our ELISA is an

appropriate primary diagnostic screening tool for human prion diseases. We think that the combination of an ELISA specific for 14-3-3 γ and the RT-QUIC method are the best diagnostic tools that can be used to detect human prion diseases in CSF.

Additional material

Additional file 1: Table S1. The profiles of all researches in the sensitivity and specificity of ELISA kits of 14-3-3 protein in CJD patients. ELISA: WB: Western blots method, N.E.: not examined We compared the previous reports of ELISA kits of 14-3-3 protein in CSF of CJD patients with our data. Supplementary reference. 1. Geschwind MD, Martindale J, Miller D et al. Challenging the clinical utility of the 14-3-3 protein for the diagnosis of sporadic Creutzfeldt-Jakob disease. *Archives of neurology*. 2003;60:813-816. 2. Kenney K, Brechtel C, Takahashi H et al. An enzyme-linked immunosorbent assay to quantify 14-3-3 proteins in the cerebrospinal fluid of suspected Creutzfeldt-Jakob disease patients. *Annals of Neurology*. 2000; 48:395-398. 3. Gmitterova K, Heinemann U, Bodemer M et al. 14-3-3 CSF levels in sporadic Creutzfeldt-Jakob disease differ across molecular subtypes. *Neurobiology of Aging*. 2009; 30(11): 1842-50.

Additional file 2: Table S2. The characterization of three monoclonal antibodies and three polyclonal antibodies in six isoforms of 14-3-3 protein. 14-3-3 proteins are a highly conserved family of multifunctional proteins which are primarily found in high levels in neurons. These proteins comprise seven distinct isoforms (β -isoform, γ -isoform, η -isoform, ϵ -isoform, ζ -isoform, τ -isoform and σ -isoform), but σ -isoform has not been detected in the human brain. We analyzed six isoforms (β -isoform, γ -isoform, η -isoform, ϵ -isoform, ζ -isoform and τ -isoform) in human CSF. We obtained the full-length gene encoding each isoform (β -isoform, γ -isoform, η -isoform, ϵ -isoform, ζ -isoform and τ -isoform) of 14-3-3 protein from a cDNA library. Full-length constructs encoding either the β - or γ -isoform of human 14-3-3 protein in addition to a His-tag were cloned into pcDNA6/His vector, after which the constructs were transfected into murine 293T cell lines and over-expressed. All isoforms of protein were collected and purified three times through an affinity chromatography column. We analyzed all isoforms of recombinant protein of 14-3-3 protein reacted by three monoclonal antibodies (#1-#3) and polyclonal antibodies (#4-#6). Two monoclonal antibodies (#1 and #2) and one polyclonal antibody (#6) were specific by only γ -isoform of 14-3-3 protein. But one monoclonal antibody (#3) and two polyclonal antibodies (#4 and #5) were reacted by other isoforms including γ -isoform of 14-3-3 protein.

Additional file 3: Figures S1a and S1b. The standard curves obtained for the sandwich ELISA (clones #1 and #6). The standard curves obtained for the sandwich ELISA (clones #1 and #6). The standard control used a recombinant γ -isoform of 14-3-3. The combination of antibodies (#1 and #6) showed a dose-dependent reaction against the γ -isoform. **Detection of 14-3-3 by the Western blot method in DAT patients.** Detection of 14-3-3 by the Western blot method in DAT patients. Both cases 1 and 2 were DAT patients. The data from the 14-3-3 ELISA indicated that the protein concentration in cases 1 and 2 were 3, 168 and 6, 773 AU/ml, respectively. The positive control (#3) was also included.

Additional file 4: Figure S2a and S2b. The relationship between the concentration of standard samples and the absorbance. The relationship between the concentration of standard samples and the absorbance. Correlation coefficient = 0.9967. **The relationship between the concentration of standard samples, and the absorbance in different standard samples.** The relationship between the concentration of standard samples, and the absorbance in different standard samples. These measurements were repeated five times. We acquired the almost data similar to the fifth.

Acknowledgements

This study was supported by the members of Research Committee of Prion disease and Slow Virus Infection from the Ministry of Health, Labour and Welfare of Japan.

This study has no industry-sponsors.

The corresponding author is responsible for ensuring that all authors agree with the Financial

Disclosure Statement.

Study funding and Funding disclaimer statement: This work was supported by: the global COE Program (F12); a grant-in-aid for science research from the Ministry of Education, Culture, Sports, Science and Technology of Japan; a grant for BSE research; and Grants-in-Aid of the Research Committee of Prion disease and Slow Virus Infection from the Ministry of Health, Labour and Welfare of Japan.

Author details

¹Department of Pharmaceutical Care and Health Sciences, Faculty of Pharmaceutical Sciences, Fukuoka University, 8-19-1 Nanakuma, Fukuoka 814-0180, Japan. ²Department of Molecular Microbiology and Immunology, Graduate School of Biomedical Science, Nagasaki University, 1-12-4 Sakamoto, Nagasaki 852-8523, Japan. ³Cyclex Co.LTD, 1063-103 Ohara, Terasawaoka, Ina, Nagano 396-0002, Japan. ⁴Center for Community and Campus Health, Nagasaki University, 1-14 Bunkyo, Nagasaki 852-8521, Japan. ⁵Nagasaki Kita Hospital, 800 Tokitsu, Nagasaki 851-2103, Japan.

Authors' contributions

YM and KM: YM and KM performed the analysis of the 14-3-3 γ ELISA, WB and tau protein ELISA for human prion disease in CSF. TM: TM made the development of a 14-3-3 γ ELISA kit and the charge nurse of the sale company of it. SS: SS is a member of the CJD Surveillance Committee in Japan from 2007 till 2011. RA: RA performed the analysis of the RT-QUIC method for detecting human prion disease in CSF. AS and YK: investigators in this study. KS: KS analyzed the 14-3-3 γ ELISA, Western blots and tau protein ELISA in CSF; KS is a member of the CJD Surveillance Committee in Japan on 2012; and chief investigator of this study. NN: NN was the chief manager of this study. All authors read and approved the final manuscript.

Competing interests

Yuki Matsui, Katsuya Satoh, Toshiaki Miyazaki, Susumu Shirabe, Ryuichiro Atarashi, Kazuo Mutsukura, Yasufumi Kataoka and Noriyuki Nishida fulfill the criteria for Conflict of Interest (COI) as determined by the conflict of interest committee of Nagasaki University and are protected by the "Policy of Conflict of Interest in Clinical Research". All authors have no disclosures and no interest in the company, entity, or organization.

Received: 22 April 2011 Accepted: 4 October 2011

Published: 4 October 2011

References

1. Hsich G, Kenney K, Gibbs CJ, Lee KH, Harrington MG: The 14-3-3 brain protein in cerebrospinal fluid as a marker for transmissible spongiform encephalopathies. *The New England journal of medicine* 1996, 335(13):924-930.
2. Brandel JP, Delasnerie-Laupretre N, Laplanche JL, Hauw JJ, Alperovitch A: Diagnosis of Creutzfeldt-Jakob disease: effect of clinical criteria on incidence estimates. *Neurology* 2000, 54(5):1095-1099.
3. Satoh K, Tobiume M, Matsui Y, Mutsukura K, Nishida N, Shiga Y, Eguhchi K, Shirabe S, Sata T: Establishment of a standard 14-3-3 protein assay of cerebrospinal fluid as a diagnostic tool for Creutzfeldt-Jakob disease. *Laboratory investigation; a journal of technical methods and pathology* 2010, 90(11):1637-1644.
4. Kenney K, Brechtel C, Takahashi H, Kurohara K, Anderson P, Gibbs CJ Jr: An enzyme-linked immunosorbent assay to quantify 14-3-3 proteins in the cerebrospinal fluid of suspected Creutzfeldt-Jakob disease patients. *Annals of neurology* 2000, 48(3):395-398.
5. Gmitterova K, Heinemann U, Bodemer M, Krasnianski A, Meissner B, Kretschmar HA, Zerr I: 14-3-3 CSF levels in sporadic Creutzfeldt-Jakob disease differ across molecular subtypes. *Neurobiology of aging* 2009, 30(11):1842-1850.

6. Satoh K, Shirabe S, Tsujino A, Eguchi H, Motomura M, Honda H, Tomita I, Satoh A, Tsujihata M, Matsuo H, *et al*: Total tau protein in cerebrospinal fluid and diffusion-weighted MRI as an early diagnostic marker for Creutzfeldt-Jakob disease. *Dementia and geriatric cognitive disorders* 2007, **24**(3):207-212.
7. Atarashi R, Satoh K, Sano K, Fuse T, Yamaguchi N, Ishibashi D, Matsubara T, Nakagaki T, Yamanaka H, Shirabe S, *et al*: Ultrasensitive human prion detection in cerebrospinal fluid by real-time quaking-induced conversion. *Nature medicine* 2011, **17**(2):175-178.
8. Chohan G, Pennington C, Mackenzie JM, Andrews M, Everington D, Will RG, Knight RS, Green AJ: The role of cerebrospinal fluid 14-3-3 and other proteins in the diagnosis of sporadic Creutzfeldt-Jakob disease in the UK: a 10-year review. *Journal of neurology, neurosurgery and psychiatry* 2010, **81**(11):1243-1248.
9. Sanchez-Juan P, Green A, Ladogana A, Cuadrado-Corrales N, Saanchez-Valle R, Mitrova E, Stoeck K, Sklaviadis T, Kulczycki J, Hess K, *et al*: CSF tests in the differential diagnosis of Creutzfeldt-Jakob disease. *Neurology* 2006, **67**(4):637-643.
10. Pennington C, Chohan G, Mackenzie J, Andrews M, Will R, Knight R, Green A: The role of cerebrospinal fluid proteins as early diagnostic markers for sporadic Creutzfeldt-Jakob disease. *Neuroscience letters* 2009, **455**(1):56-59.

Pre-publication history

The pre-publication history for this paper can be accessed here:
<http://www.biomedcentral.com/1471-2377/11/120/prepub>

doi:10.1186/1471-2377-11-120

Cite this article as: Matsui *et al*: High sensitivity of an ELISA kit for detection of the gamma-isoform of 14-3-3 proteins: usefulness in laboratory diagnosis of human prion disease. *BMC Neurology* 2011 **11**:120.

**Submit your next manuscript to BioMed Central
and take full advantage of:**

- Convenient online submission
- Thorough peer review
- No space constraints or color figure charges
- Immediate publication on acceptance
- Inclusion in PubMed, CAS, Scopus and Google Scholar
- Research which is freely available for redistribution

Submit your manuscript at
www.biomedcentral.com/submit



Co-Occurrence of Types 1 and 2 PrP^{res} in Sporadic Creutzfeldt-Jakob Disease MM1

Atsushi Kobayashi,* Kenta Mizukoshi,*
Yasushi Iwasaki,[†] Hajime Miyata,[‡]
Yasuji Yoshida,[‡] and Tetsuyuki Kitamoto*

From the Division of Neurological Science, Center for Prion Research, Tohoku University Graduate School of Medicine, Sendai; the Department of Neurology,[†] Oyamada Memorial Spa Hospital, Yokkaichi; and the Department of Neuropathology,[‡] Research Institute for Brain and Blood Vessels–Akita, Akita, Japan*

The genotype (M/M, M/V, or V/V) at polymorphic codon 129 of the human prion protein (PrP) gene and the type (1 or 2) of protease-resistant PrP (PrP^{res}) in the brain are major determinants of the clinicopathological phenotypes of sporadic Creutzfeldt-Jakob disease (sCJD). According to this molecular typing system, sCJD has been classified into six subgroups (MM1, MM2, MV1, MV2, VV1, and VV2). Besides these pure subgroups, mixed cases presenting mixed neuropathological phenotypes and more than one PrP^{res} type have been found in sCJD. To investigate the frequency of the co-occurrence of types 1 and 2 PrP^{res} in sCJD patients classified as MM1, we produced type 2 PrP^{res}-specific antibody Tohoku 2 (T2) that can specifically detect the N-terminal cleavage site of type 2 PrP^{res} after protease treatment and examined brain samples from 23 patients with sCJD-MM1. Western blot analysis using the T2 antibody revealed that the minority type 2 PrP^{res} could be detected in all sCJD-MM1 brain samples including those of the cerebellum where sCJD-MM2 prions rarely accumulate. These results show that the co-occurrence of types 1 and 2 PrP^{res} within a single sCJD-MM1 patient is a universal phenomenon. The general co-occurrence of multiple PrP^{res} fragments within a single prion strain questions the validity of the conventional molecular typing system. (*Am J Pathol* 2011, 178:1309–1315; DOI: 10.1016/j.ajpath.2010.11.069)

Creutzfeldt-Jakob disease (CJD) is a lethal transmissible neurodegenerative disease caused by an abnormal isoform of prion protein (PrP^{Sc}), which is converted from the

normal cellular isoform (PrP^C).¹ The genotype (M/M, M/V, or V/V) at polymorphic codon 129 of the human prion protein (PrP) gene and the type (type 1 or type 2) of PrP^{Sc} in the brain are major determinants of the clinicopathological phenotypes of sporadic CJD (sCJD).^{2–5} Type 1 and type 2 PrP^{Sc} are distinguishable according to the size of the proteinase K (PK)-resistant core of PrP^{Sc} (PrP^{res}) (21 and 19 kDa, respectively), reflecting differences in the PK-cleavage site (at residues 82 and 97, respectively).^{2,5} According to this molecular typing system, sCJD has been classified into six subgroups (MM1, MM2, MV1, MV2, VV1, or VV2).

Besides these “pure” subgroups, “mixed” cases presenting mixed neuropathological phenotypes and more than one PrP^{res} type have been reported.^{4,6–10} At first, the co-occurrence of types 1 and 2 PrP^{res} within one individual was found in five of 14 patients with sCJD.⁶ Recently, a systematic regional study in a series of 225 patients revealed that 35% of the sCJD patients presented both PrP^{res} types.⁹ In addition to these neuropathologically and biochemically mixed cases, monoclonal antibodies recognizing an epitope between residues 82 and 96 of human PrP (ie, specifically detecting type 1 PrP^{res} after PK digestion), revealed that all CJD patients formerly classified as type 2 contained the minority type 1 PrP^{res} despite the lack of mixed neuropathological phenotypes.^{11,12} The co-occurrence of multiple PrP^{res} fragments without mixed neuropathological phenotypes has remained controversial. To investigate accurately the frequency of the co-occurrence of types 1 and 2 PrP^{res}, we produced type 2 PrP^{res}-specific polyclonal antibody Tohoku 2 (T2)¹³ and examined brain samples from 23 patients formerly classified as sCJD-MM1. Here we report

Supported by Grants-in-Aid from the Research Committee of Prion disease and Slow Virus Infection, the Ministry of Health, Labour and Welfare of Japan (A.K., Y.I., and T.K.), and by Grants-in-Aid for Scientific Research from the Ministry of Education, Culture, Sports, Science and Technology of Japan (A.K. and T.K.).

Accepted for publication November 24, 2010.

Address reprint requests to Tetsuyuki Kitamoto, Ph.D., Division of Neurological Science, Center for Prion Diseases, Tohoku University Graduate School of Medicine, 2-1 Seiryō-machi, Aoba-ku, Sendai 980-8575, Japan. E-mail: kitamoto@med.tohoku.ac.jp.

Table 1. Summary of Clinical Features

	Age at onset (years)	PSWC on EEG (months)	Myoclonus (months)*	Akinetic mutism (months)*	Duration of illness (months)	PrP deposition
MM1 (<i>n</i> = 23)	68.6 ± 7.8	2.0 ± 2.6 (23/23) [†]	2.2 ± 2.5 (23/23) [†]	3.0 ± 3.2	13.5 ± 7.8	Synaptic
MM1+2 (<i>n</i> = 9)	65.8 ± 10.2	5.3 ± 5.8 (8/9) [†]	4.8 ± 5.4 (9/9) [†]	5.7 ± 6.3	11.8 ± 10.9	Synaptic + perivacuolar

Values are mean ± SD.

*Duration until appearance of PSWC, myoclonus, or akinetic mutism from onset.

[†]Positive rate.

that the minority type 2 PrP^{res} could be detected with type 1 in all sCJD-MM1 patients examined.

Materials and Methods

Patients

All CJD cases included in this study were patients with clinically, genetically, and neuropathologically proven sCJD. The diagnosis of CJD and the type of PrP^{res} were confirmed by neuropathological examination, PrP immunohistochemistry, and conventional Western blotting using monoclonal antibody 3F4 as described.^{14,15} The genotype and the absence of mutations in the open reading frame of the PrP gene were determined by sequence analysis.¹⁶ All subjects were homozygous for methionine at codon 129 of the PrP gene and were classified as follows: MM1, 23 cases; MM1+2 (MM1-dominant form), nine cases; MM2 (cortical form), one case. The clinical features of the patients are summarized in Table 1. Detailed information of this sCJD-MM2 patient has been reported previously.¹⁷ Four age-matched control subjects were included in this study and were also homozygous for methionine at codon 129 of the PrP gene.

Sample Preparation and Western Blotting

Brain tissues were obtained at autopsy from the patients after receiving informed consent for research use. PrP^{res} was extracted from brain tissues with collagenase treatment as described¹⁸ with some modifications. Samples were subjected to 13% SDS–polyacrylamide gel electrophoresis and Western blotting as described.¹⁹ The production of type 2 PrP^{res}-specific polyclonal antibody T2 has been reported previously.¹³ The monoclonal antibody 3F4²⁰ and the T2 antibody were used as the primary antibodies. Goat–antimouse immunoglobulin polyclonal antibody labeled with the peroxidase-conjugated dextran polymer, EnVision+ (Dako, Carpinteria, CA) and antirabbit EnVision+ were used as the secondary antibodies. The signal intensities of the Western blots were quantified with Quantity One software using an imaging device, VersaDoc 5000 (Bio-Rad Laboratories, Hercules, CA).

Immunohistochemistry

Formalin-fixed brain tissues were treated with 99% formic acid for 1 hour to inactivate the infectivity and embedded

in paraffin. Tissue sections were pretreated by hydrolytic autoclaving before PrP immunohistochemistry.¹⁴ The 3F4 antibody and the monoclonal antibody #71^{21,22} were used as the primary antibodies. Antimouse EnVision+ was used as the secondary antibody.

Results

T2-Reactive PrP^{res} Fragments in the Cerebrums from sCJD-MM1 Patients

To determine whether type 2 PrP^{res} could be detected in the sCJD patients formerly classified as type 1, we examined the cerebral samples from 23 patients with sCJD-MM1 by Western blotting using type 2 PrP^{res}-specific polyclonal antibody T2 (Figure 1A). The T2 antibody is a proteolytic cleavage site–specific antibody and can specifically react with the N-terminally cleaved type 2 PrP^{res} after PK digestion.¹³ Although the N-terminal cleavage of type 2 PrP^{res} by PK treatment can occur at several sites,⁵ the T2 antibody detects the major cleavage products cleaved at residue 97.¹³ As the positive control for the T2 antibody, we also examined nine patients with sCJD-MM1+2 (MM1-dominant form) and one patient with sCJD-MM2 (cortical form). In the conventional Western blot analysis using the monoclonal antibody 3F4, which is the most popular anti-PrP antibody that reacts with all PrP^{res} types, the sCJD-MM1 brains showed only type 1 PrP^{res} (Figure 1B). In contrast, in the Western blot analysis using the T2 antibody, all sCJD-MM1 brains contained T2-reactive PrP^{res} fragments (Figure 1C). The sizes of the T2-reactive fragments were identical to those of type 2 PrP^{res} in the sCJD-MM2 brain. In the quantitative analysis, the mean signal intensities of PrP^{res} in the sCJD-MM2 brain were assigned as 100/mm² in each experiment using the 3F4 or T2 antibody (Figure 1D). To compare the amounts of the T2-reactive PrP^{res} fragments among the patients, the mean signal intensities of the T2-reactive fragments were divided by those of the 3F4-reactive PrP^{res} fragments, and the percentage of the T2-reactive fragments was calculated in each case (T2/3F4 ratio). The mean T2/3F4 ratio of the sCJD-MM1 patients was significantly lower than that of the sCJD-MM1+2 patients (Figure 1E). Thus, small but significant amounts of T2-reactive PrP^{res} fragments could be detected in all sCJD-MM1 patients examined.

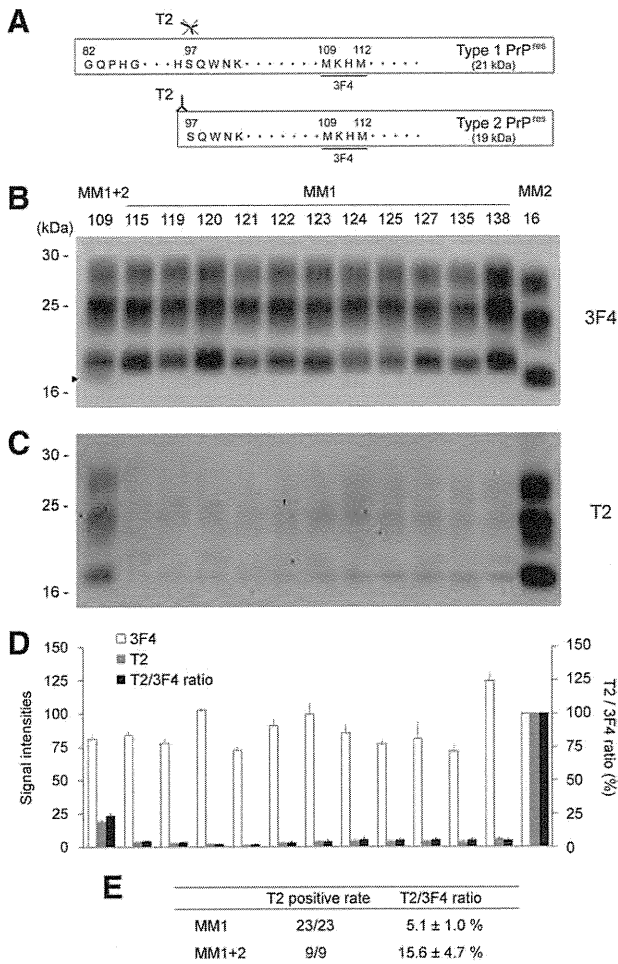


Figure 1. Tohoku 2 (T2)-reactive PrP^{res} fragments in the cerebrums from sCJD-MM1 patients. **A:** The epitope for type 2 PrP^{res}-specific antibody T2. The T2 antibody specifically detects the N-terminal cleavage site of type 2 PrP^{res}.¹⁵ In contrast, 3F4 antibody detects both PrP^{res} types. **B:** The conventional Western blot analysis using the 3F4 antibody was used for the classification of sCJD patients included in this study. The subgroup and case number of each patient are described above each lane. A faint type 2 PrP^{res} band (arrowhead) was detected with the majority type 1 PrP^{res} bands in the sCJD-MM1+2 brain (case 109). **C:** T2-reactive PrP^{res} fragments could be detected in all sCJD-MM1 brains examined. **D:** The signal intensities of the 3F4-reactive PrP^{res} fragments (white bars) or those of the T2-reactive PrP^{res} fragments (gray bars). The mean signal intensities of PrP^{res} in the sCJD-MM2 brain (case 16) were assigned as 100/mm² in each experiment. To compare the amounts of the T2-reactive PrP^{res} fragments among the patients, the mean signal intensities of the T2-reactive fragments were divided by those of the 3F4-reactive fragments, and the percentage of the T2-reactive fragments was calculated in each case (T2/3F4 ratio, black bars). The data are expressed as mean ± SEM (*n* = 3). **E:** Summary of the Western blot analysis using the T2 antibody. Values are means ± SEM.

T2-Reactive PrP^{res} Fragments in the Cerebellums from sCJD-MM1 Patients

The consistent detection of the T2-reactive PrP^{res} fragments in the cerebrums from sCJD-MM1 patients led us to suppose that co-occurrence of types 1 and 2 PrP^{res} fragments might be a universal phenomenon. Indeed, the T2-reactive PrP^{res} fragments were also detected in the cerebellum of a sCJD-MM1+2 patients in the present study. In most sCJD-MM1+2 patients, type 2 PrP^{res} is rarely detected in the cerebellum by conventional Western blot analysis.⁹ In addition, the cerebellums from

sCJD-MM1+2 patients lack the perivacuolar PrP deposition that is characteristic of sCJD-MM2 prions, whereas the cerebrums show a mixed PrP deposition pattern (ie, synaptic plus perivacuolar PrP deposition).^{9,10} In accordance with these reports, the cerebellums from the sCJD-MM1+2 patients in the present study lacked perivacuolar PrP deposition and showed only the synaptic-type PrP deposition, whereas the cerebral cortices showed perivacuolar PrP deposition in addition to the synaptic-type PrP deposition (Figure 2A). Furthermore, conventional Western blot analysis using the 3F4 antibody showed the lack of type 2 PrP^{res} accumulation in the cerebellum of the sCJD-

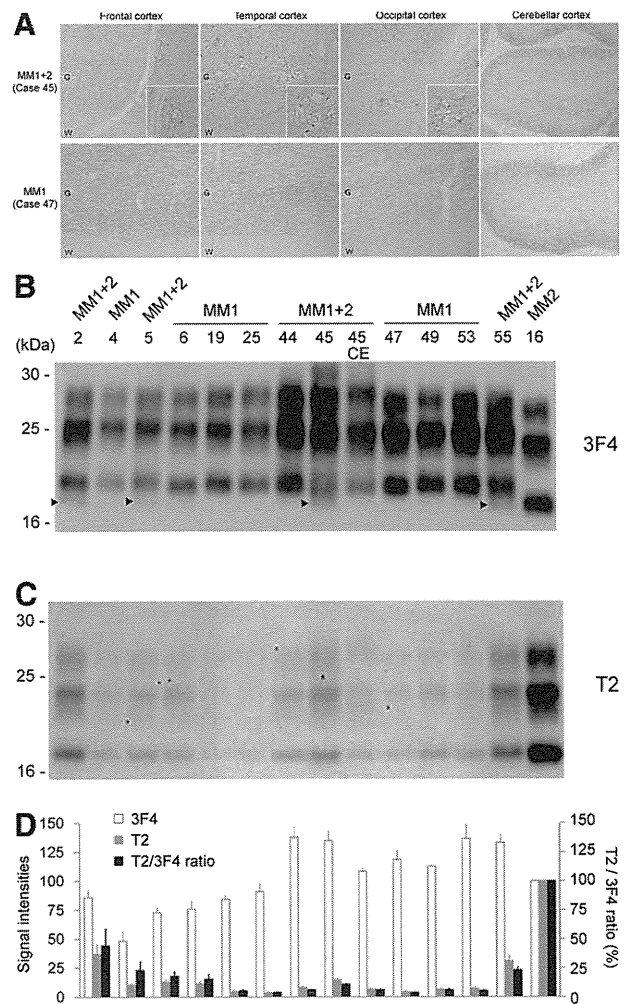


Figure 2. T2-reactive PrP^{res} fragments in the cerebellum from the sCJD-MM1+2 patient. **A:** Immunohistochemistry using the anti-PrP antibody #71 showed that perivacuolar PrP deposition was restricted to within the cerebral cortices in the sCJD-MM1+2 patient (cases 45; ×40, insets ×200). The sCJD-MM1 patient showed only synaptic-type PrP deposition (case 47; ×40). G = gray matter; W = white matter. **B:** In the conventional Western blot analysis using the 3F4 antibody, faint type 2 PrP^{res} bands (arrowheads) were detected in the cerebrums from the sCJD-MM1+2 patients (cases 2, 5, 45, and 55) but not in the cerebellum (case 45 CE). In case 44, although neuropathological examination showed focal perivacuolar PrP deposition, the conventional Western blot analysis failed to detect type 2 PrP^{res}. **C:** T2-reactive PrP^{res} fragments could be detected also in the cerebellum of the sCJD-MM1+2 patient (case 45 CE). **D:** The signal intensities of the 3F4-reactive PrP^{res} fragments (white bars) or those of the T2-reactive PrP^{res} fragments (gray bars), and the T2/3F4 ratios (black bars). The mean signal intensities of PrP^{res} in the sCJD-MM2 brain (case 16) were assigned as 100/mm² in each experiment. Data are expressed as mean ± SEM (*n* = 3).

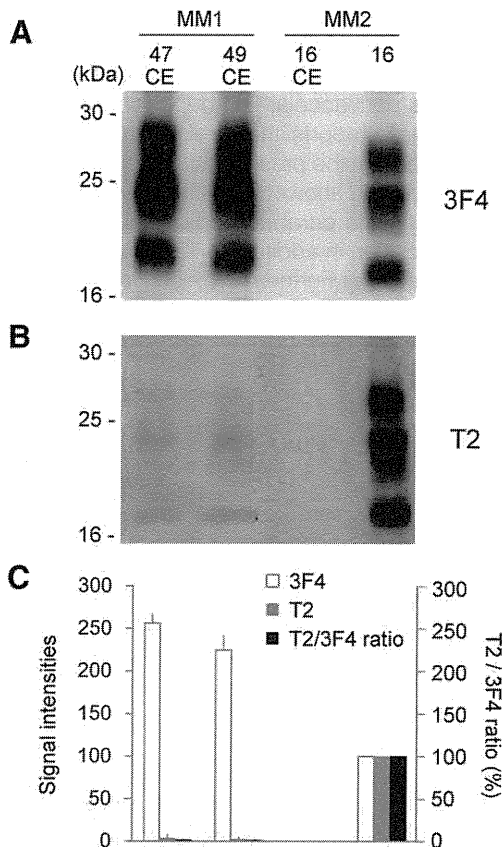


Figure 3. T2-reactive PrP^{res} fragments in the cerebellums from the sCJD-MM1 patients. **A:** In the conventional Western blot analysis using the 3F4 antibody, PrP^{res} was not detected in the cerebellum of the sCJD-MM2 patient (case 16 CE). **B:** The T2-reactive PrP^{res} fragments could be detected in the cerebellums from the sCJD-MM1 patients (cases 47 CE and 49 CE), but not in the cerebellum from the sCJD-MM2 patient (case 16 CE). **C:** The signal intensities of the 3F4-reactive PrP^{res} fragments (white bars) or those of the T2-reactive PrP^{res} fragments (gray bars), and the T2/3F4 ratios (black bars). The mean signal intensities of PrP^{res} in the sCJD-MM2 cerebrum (case 16) were assigned as 100/mm² in each experiment. Data are expressed as mean \pm SEM ($n = 3$).

MM1+2 patient (case 45 CE) (Figure 2B). Nevertheless, Western blot analysis using the T2 antibody revealed that the cerebellum of the sCJD-MM1+2 patient (case 45 CE) contained T2-reactive PrP^{res} fragments (Figure 2C). The sizes of the T2-reactive fragments were identical to those of type 2 PrP^{res} in the sCJD-MM2 brain. In the quantitative analysis, the T2/3F4 ratio of the cerebellum (case 45 CE) was lower than that of the cerebrum (case 45) (Figure 2D). Thus, small amounts of T2-reactive PrP^{res} fragments could be detected also in the cerebellum of the sCJD-MM1+2 patients.

For further analysis, we also examined the cerebellums from two sCJD-MM1 patients. In most sCJD-MM2 patients, the cerebellum lacks significant pathology, and PrP deposition is seldom or never observed.⁴ In line with this report, the cerebellum of the present sCJD-MM2 patient (case 16 CE) did not contain any PrP^{res} signals when probed with the 3F4 or T2 antibody (Figure 3, A and B).¹⁷ In contrast, the cerebellums from the sCJD-MM1 patients contained the T2-reactive PrP^{res} fragments (cases 47 CE and 49 CE). These T2-reactive PrP^{res} fragments showed the exact type 2 PrP^{res} migration pattern. In the quantitative analysis, the T2/3F4 ratios of the

cerebellums (case 47 CE, 1.5% \pm 0.8%; case 49 CE, 1.1% \pm 0.5%) were lower than those of the cerebrums (case 47, 3.4% \pm 0.5%; case 49, 5.9% \pm 0.8%) (Figure 3C). Thus, trace amounts of T2-reactive PrP^{res} fragments could be detected in all sCJD-MM1 brain samples including those of the cerebellum.

T2-Reactive Truncated PrP^C Fragments in Non-CJD Control Brains

The normal cellular isoform of PrP, denoted as PrP^C, is cleaved by endogenous proteases and can generate various N-terminally truncated PrP^C molecules.^{23,24} This raised the possibility that T2-reactive PrP^C fragments (97-PrP^C) might pre-exist in the brains and might be incorporated into MM1 PrP^{res} aggregates in sCJD-MM1 patients. To determine whether the 97-PrP^C fragments can be generated in normal brains, we examined brain samples from four age-matched control subjects without PK treatment. Western blot analysis using the T2 antibody showed that the cerebral cortices from the control subjects contained 97-PrP^C (Figure 4, A and B). The glycosylation patterns of these 97-PrP^C fragments were different from those of the T2-reactive PrP^{res} fragments observed in the sCJD patients. After deglycosylation with PNGase F, these 97-PrP^C fragments migrated at 19 kDa. Moreover, the cerebellums from the control subjects also contained the 97-PrP^C (Figure 4, C and D). Thus, the T2-reactive truncated PrP^C fragments could be detected in all control brain samples including those of the cerebellums.

Patchy Plaque-Type PrP Deposition in the sCJD-MM1 Patients with High T2/3F4 Ratios

In the 23 patients with sCJD-MM1 examined in the present study, two patients (cases 4 and 6) showed high T2/3F4 ratios similar to those of the sCJD-MM1+2 patients (Figure 2D). The clinical courses of cases 4 and 6 were not significantly different from those of the other sCJD-MM1 patients (Figure 5A). Indeed, the duration until the appearance of akinetic mutism and total duration of illness in case 6 were rather shorter than the mean values in the sCJD-MM1 patients. However, the high T2/3F4 ratios raised the possibility that these two sCJD patients might contain a focal deposition of MM2 prions overlooked in the previous examination. Therefore, we re-examined all brain sections from these patients by PrP immunohistochemistry. The cerebral and cerebellar cortices from the two patients lacked perivacuolar PrP deposition and showed diffuse synaptic-type PrP deposition. However, careful re-examination revealed a very focal accumulation of small PrP plaques in the cerebral cortices (Figure 5B). These patchy plaque-type PrP deposits were not accompanied by large vacuoles, in contrast to the perivacuolar PrP deposition (Figure 5, C and D). Meanwhile, besides perivacuolar and synaptic-type deposition, coarse PrP deposits similar to the patchy plaque-type PrP deposition were observed in the cerebral cortices from the sCJD-MM1+2 patients. These coarse PrP deposits in the sCJD-MM1+2 patients were

also independent of vacuoles (Figure 5E). Thus, the sCJD-MM1 patients with the high T2/3F4 ratios showed the patchy plaque-type PrP deposition similar to the coarse PrP deposition in the sCJD-MM1+2 patients. Although these sCJD patients had been classified into MM1 by the conventional classification system because the lack of perivacuolar PrP deposition, the patchy plaque-type PrP deposition might indicate the existence of MM2 prions.

Discussion

Our data comprised three major findings. First, using the novel antibody T2 that can specifically react with the N-terminal cleavage site of type 2 PrP^{res} after PK digestion, type 2 PrP^{res} could be detected in all sCJD-MM1 brain samples including those of the cerebellum where sCJD-MM2 prions rarely accumulate. Second, T2-reactive truncated PrP^C fragments (97-PrP^C) could be detected in

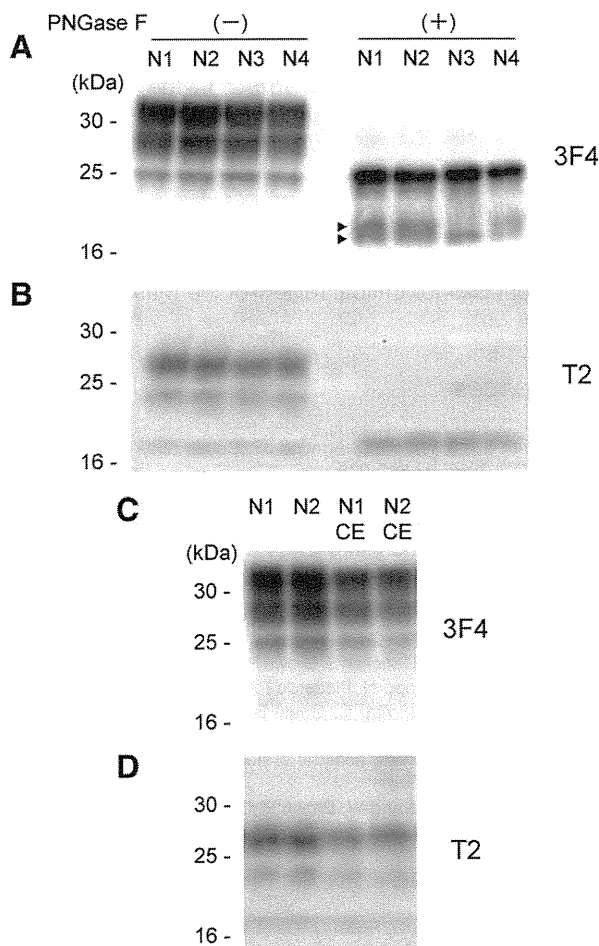


Figure 4. T2-reactive truncated PrP^C fragments in non-CJD control brains. **A:** The cerebral cortices from age-matched control subjects (N1 to N4) were examined by conventional Western blot analysis using the 3F4 antibody without PK treatment. After deglycosylation with PNGase F, major PrP^C fragments migrated at 25 kDa. In addition, various truncated PrP^C fragments (**arrowheads**) were also observed. **B:** T2-reactive truncated PrP^C fragments (97-PrP^C) could be detected in all control brains. The 97-PrP^C fragments migrated at 19 kDa after the deglycosylation. **C** and **D:** The 97-PrP^C fragments could be detected also in the cerebellums from the control subjects (N1 CE and N2 CE).

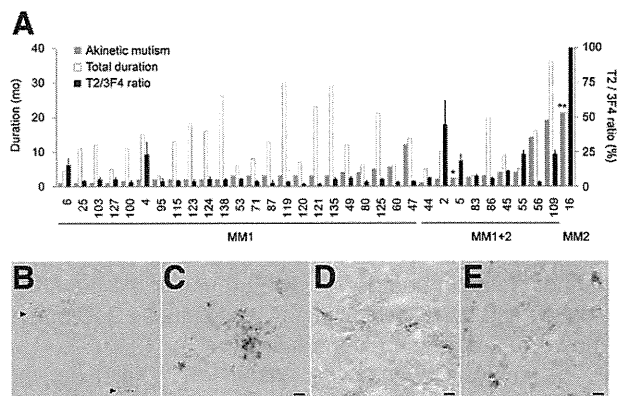


Figure 5. Patchy plaque-type PrP deposition in the sCJD-MM1 patients with high T2/3F4 ratios. **A:** The duration until the appearance of akinetic mutism (gray bars), total duration of illness (white bars), and the T2/3F4 ratio (black bars) of the sCJD patients. The sCJD-MM1 or sCJD-MM1+2 cases are arranged in order of the duration until the appearance of akinetic mutism. *The patient became unconsciousness and bedridden 1 month after the initial symptom because of respiratory failure. **The patient did not present akinetic mutism throughout the clinical course. **B:** PrP immunohistochemistry using the 3F4 antibody revealed patchy plaque-type PrP deposition (**arrowheads**) besides diffuse synaptic-type PrP deposition in the cerebral cortices from the sCJD-MM1 patient with the high T2/3F4 ratio (case 4; temporal cortex; $\times 40$). **C:** The patchy plaque-type PrP deposition was independent of vacuoles (case 4; occipital cortex; $\times 400$). **D:** The patchy plaque-type deposition in the other sCJD-MM1 patient with the high T2/3F4 ratio (case 6; frontal cortex; $\times 400$). **E:** The cerebral cortices from the sCJD-MM1+2 patient showed coarse PrP deposition similar to the patchy plaque-type PrP deposition (case 5; parietal cortex; $\times 400$). Scale bars = 10 μ m.

age-matched control brains without PK treatment. Third, two sCJD-MM1 patients with relatively high type 2 PrP^{res} contents showed unique PrP deposition, namely the patchy plaque-type deposition. Here we demonstrate that the co-occurrence of types 1 and 2 PrP^{res} within a single sCJD-MM1 patient is a universal phenomenon.

The trace amounts of type 2 PrP^{res} in the sCJD-MM1 brains might result from the involvement of 97-PrP^C fragments into the MM1 PrP^{res} aggregates. Despite the lack of perivacuolar PrP deposition that is characteristic of sCJD-MM2 prions, trace amounts of type 2 PrP^{res} were detected in all sCJD-MM1 patients examined. In addition, type 2 PrP^{res} could be detected not only in the cerebrums but also in the cerebellums where sCJD-MM2 prions rarely accumulate. These findings support the view of the co-occurrence of multiple PrP^{res} fragments within MM1 prions rather than the co-occurrence of multiple prion strains within the same individual. One possible explanation for the co-occurrence of multiple PrP^{res} fragments within a single prion strain is the involvement of multiple PrP^C fragments into the PrP^{res} aggregates. There is accumulating evidence that various N-terminally truncated PrP^C molecules exist in human brains.^{23,24} Moreover, T2-reactive 97-PrP^C fragments existed in normal human brains in the present study. These 97-PrP^C fragments might be incorporated into the PrP^{res} aggregates with full-length PrP^{Sc} and might acquire protease resistance as reported in deletion mutant PrPs or green fluorescent protein-tagged PrP.^{25,26} These findings lead us to speculate that the minority type 1 PrP^{res} detected in the brains from CJD patients classified as type 2^{11,12} might also be caused by the involvement of 82-PrP^C fragments. Because the type 1 PrP^{res}-specific antibodies used in these

reports recognize an epitope between residues 82 and 96 of human PrP and can react with full-length PrP^C, it remains to be determined whether 82-PrP^C fragments can be generated in human brains. If an antibody that can specifically detect the N-terminal cleavage site at residue 82 is generated, 82-PrP^C fragments might also be detected in human brains. To examine the possibility of the co-occurrence of multiple prion strains within one individual, whether transmissibilities and pathological phenotypes can be split into two groups in the transmission studies using the limiting dilution of these CJD brains should be addressed in the future.

The analysis of the type 2/total PrP^{res} ratio (ie, the T2/3F4 ratio) using the T2 antibody may have significance in classifications of sCJD. In the present study, two of 23 sCJD-MM1 patients showed high T2/3F4 ratios and the unique PrP deposition designated as the patchy plaque-type. Because the patchy plaque-type deposition was similar to the coarse PrP deposition in the sCJD-MM1+2 patients, these deposits might be precursors of the perivacuolar PrP deposition or variant deposition patterns of MM2 prions. The finding of the patchy plaque-type deposition in the sCJD patients who have been neuropathologically and biochemically classified into MM1 raises the possibility that the co-occurrence of MM1 and MM2 prions within the same brain might be underestimated in the conventional classification. Hereafter, sCJD-MM1 patients need to be examined by the T2 antibody, and the focal accumulation of MM2 prions must be tested carefully in patients showing high T2/3F4 ratios compared with the mean value of the sCJD-MM1 patients (5.1%). On the other hand, although the mean T2/3F4 ratio of the sCJD-MM1+2 patients was significantly higher than that of the sCJD-MM1 patients, some of the sCJD-MM1+2 patients showed low T2/3F4 ratios indistinguishable from those of the sCJD-MM1 patients. These results suggest that examination using the T2 antibody is insufficient to discriminate sCJD-MM1+2 from sCJD-MM1 when the amount of type 2 PrP^{res} is marginal and the examined brain region is limited. To avoid missing the focal accumulation of MM2 prions, multiple brain regions need to be examined by the T2 antibody, as suggested when using the conventional Western blot analysis.⁹

Unfortunately, immunohistochemical analysis of type 2 PrP^{res} using the T2 antibody was unavailable in the present study. To eliminate the infectivity of sCJD prions, all brain sections had to be treated with formic acid, and infectious conformers were denatured. Therefore, the PrP^{res} type-specific cleavage by PK treatment was impossible in tissue sections. We also attempted to detect the endogenous protease-cleaved type 2 PrP^{res} without PK treatment. In this preliminary experiment, the patchy plaque-type PrP deposition in the sCJD-MM1 patients with the high T2/3F4 ratios showed the T2-immunoreactivities, whereas the synaptic-type deposition was not immunolabeled with the T2 antibody (A. Kobayashi and T. Kitamoto, unpublished). However, as 97-PrP^C fragments also exist in human brains, we cannot conclude whether the T2 immunoreactivities observed in the sCJD

brains without PK treatment represent the existence of type 2 PrP^{res}.

In conclusion, the present study, together with evidence from other groups,^{11,12} suggests that the co-occurrence of multiple PrP^{res} fragments within a single sCJD patient is a universal phenomenon. These findings show that the conventional typing of PrP^{res} merely represents the predominant PrP^{res} subpopulation among multiple co-existing PrP^{res} fragments. Besides the general co-occurrence of multiple PrP^{res} fragments, the condition of PK digestion easily affects the size of PrP^{res}.^{27,28} Indeed, insufficient PK digestion can generate type 1 PrP^{res}-specific antibody-reactive fragments in the sCJD patients classified as type 2.²⁹ Furthermore, it is possible that the conventional Western blot analysis fails to detect type 2 PrP^{res} in sCJD-MM1+2 cases showing very focal perivacuolar PrP deposition in the brain.⁹ These confusing aspects of PrP^{res} typing question the validity of the conventional molecular typing system. For a precise classification, it may be appropriate that the neuropathological phenotyping [synaptic (SY), perivacuolar (PV), plaque (PL), or patchy plaque (PP)] be combined with the molecular typing [eg, sCJD-MM1(+2)/SY+PV] the sCJD-MM patient showing synaptic + perivacuolar PrP deposition, but not type 2 PrP^{res} in the conventional Western blot analysis.

Acknowledgments

We thank Hiroko Kudo for excellent technical assistance and Brent Bell for critical review of the manuscript.

References

1. Prusiner SB, Scott MR, DeArmond JP, Cohen FE: Prion protein biology. *Cell* 1998, 93:337–348
2. Parchi P, Castellani R, Capellari S, Ghetti B, Young K, Chen SG, Farlow M, Dickson DW, Sima AA, Trojanowski JQ, Petersen RB, Gambetti P: Molecular basis of phenotypic variability in sporadic Creutzfeldt-Jakob disease. *Ann Neurol* 1996, 39:767–778
3. Parchi P, Capellari S, Chen SG, Petersen RB, Gambetti P, Kopp N, Brown P, Kitamoto T, Tateishi J, Giese A, Kretzschmar H: Typing prion isoforms. *Nature* 1997, 386:232–234
4. Parchi P, Giese A, Capellari S, Brown P, Schulz-Schaeffer W, Windl O, Zerr I, Budka H, Kopp N, Piccardo P, Poser S, Rojiani A, Streichenberger N, Julien J, Vital C, Ghetti B, Gambetti P, Kretzschmar H: Classification of sporadic Creutzfeldt-Jakob disease based on molecular and phenotypic analysis of 300 subjects. *Ann Neurol* 1999, 46:224–233
5. Parchi P, Zou W, Wang W, Brown P, Capellari S, Ghetti B, Kopp N, Schulz-Schaeffer WJ, Kretzschmar HA, Head MW, Ironside JW, Gambetti P, Chen SG: Genetic influence on the structural variations of the abnormal prion protein. *Proc Natl Acad Sci USA*: 2000, 97:10168–10172
6. Puoti G, Giaccone G, Rossi G, Canciani B, Bugiani O, Tagliavini F: Sporadic Creutzfeldt-Jakob disease: co-occurrence of different types of PrP^{Sc} in the same brain. *Neurology* 1999, 53:2173–2176
7. Schoch G, Seeger H, Bogousslavsky J, Tolnay M, Janzer RC, Aguzzi A, Glatzel M: Analysis of prion strains by PrP^{Sc} profiling in sporadic Creutzfeldt-Jakob disease. *PLoS One* 2006, 3:e14
8. Uro-Coste E, Cassard H, Simon S, Lugan S, Bilheude JM, Perret-Liaudet A, Ironside JW, Haik S, Basset-Leobon C, Lacroux C, Peoch K, Streichenberger N, Langeveld J, Head MW, Grassi J, Hauw JJ, Schelcher F, Delisle MB, Andréoletti O: Beyond PrP^{res} type 1 / type 2

- dichotomy in Creutzfeldt-Jakob disease. *PLoS Pathog* 2008, 4:e1000029
9. Parchi P, Strammiello R, Notari S, Giese A, Langeveld JP, Ladogana A, Zerr I, Roncaroli F, Cras P, Ghetti B, Pocchiari M, Kretzschmar H, Capellari S: Incidence and spectrum of sporadic Creutzfeldt-Jakob disease variants with mixed phenotype and co-occurrence of PrP^{Sc} types: an updated classification. *Acta Neuropathol* 2009, 118: 659–671
 10. Cali I, Castellani R, Alshekhlee A, Cohen Y, Blevins J, Yuan J, Langeveld JP, Parchi P, Safar JG, Zou WQ, Gambetti P: Co-existence of scrapie prion protein types 1 and 2 in sporadic Creutzfeldt-Jakob disease: its effect on the phenotype and prion-type characteristics. *Brain* 2009, 132:2643–2658
 11. Polymenidou M, Stoock K, Glatzel M, Vey M, Bellon A, Aguzzi A: Coexistence of multiple PrP^{Sc} types in individuals with Creutzfeldt-Jakob disease. *Lancet Neurol* 2005, 4:805–814
 12. Yull HM, Ritchie DL, Langeveld JPM, van Zijderdeld FG, Bruce ME, Ironside JW, Head MW: Detection of type 1 prion protein in variant Creutzfeldt-Jakob disease. *Am J Pathol* 2006, 168:151–157
 13. Kobayashi A, Sakuma N, Matsuura Y, Mohri S, Aguzzi A, Kitamoto T: Experimental verification of a traceback phenomenon in prion infection. *J Virol* 2010, 84:3230–3238
 14. Kitamoto T, Shin R-W, Doh-ura K, Tomokane N, Miyazono M, Muramoto T, Tateishi J: Abnormal isoform of prion proteins accumulates in the synaptic structures of the central nervous system in patients with Creutzfeldt-Jakob disease. *Am J Pathol* 1992, 140: 1285–1294
 15. Taguchi Y, Mohri S, Ironside JW, Muramoto T, Kitamoto T: Humanized knock-in mice expressing chimeric prion protein showed varied susceptibility to different human prions. *Am J Pathol* 2003, 163:2585–2593
 16. Kitamoto T, Ohta M, Doh-ura K, Hitoshi S, Terao Y, Tateishi J: Novel missense variants of prion protein in Creutzfeldt-Jakob disease or Gerstmann-Sträussler syndrome. *Biochem Biophys Res Commun* 1993, 191:709–714
 17. Nozaki I, Hamaguchi T, Noguchi-Shinohara M, Ono K, Shirasaki H, Komai K, Kitamoto T, Yamada M: The MM2-cortical form of sporadic Creutzfeldt-Jakob disease presenting with visual disturbance. *Neurology* 2006, 67:531–533
 18. Grathwohl KU, Horiuchi M, Ishiguro N, Shinagawa M: Improvement of PrP^{Sc}-detection in mouse spleen early at the preclinical stage of scrapie with collagenase-completed tissue homogenization and Sarkosyl-NaCl extraction of PrP^{Sc}. *Arch Virol* 1996, 141:1863–1874
 19. Asano M, Mohri S, Ironside JW, Ito M, Tamaoki N, Kitamoto T: vCJD prion acquires altered virulence through trans-species infection. *Biochem Biophys Res Commun* 2006, 342:293–299
 20. Kascsak RJ, Rubenstein R, Merz PA, Tonna-DeMasi M, Fersko R, Carp RI, Wisniewski HM, Diringer H: Mouse polyclonal and monoclonal antibody to scrapie-associated fibril proteins. *J Virol* 1987, 61: 3688–3693
 21. Muramoto T, Tanaka T, Kitamoto N, Sano C, Hayashi Y, Kutomi T, Yutani C, Kitamoto T: Analyses of Gerstmann-Straussler syndrome with 102Leu219Lys using monoclonal antibodies that specifically detect human prion protein with 219Glu. *Neurosci Lett* 2000, 288:179–182
 22. Satoh K, Muramoto T, Tanaka T, Kitamoto N, Ironside JW, Nagashima K, Yamada M, Sato T, Mohri S, Kitamoto T: Association of an 11–12 kDa protease-resistant prion protein fragment with subtypes of dura graft-associated Creutzfeldt-Jakob disease and other prion diseases. *J Gen Virol* 2003, 84:2885–2893
 23. Chen SG, Teplow DB, Parchi P, Teller JK, Gambetti P, Auttilio-Gambetti L: Truncated forms of the human prion protein in normal brain and in prion diseases. *J Biol Chem* 1995, 270:19173–19180
 24. Jiménez-Huete A, Lievens PM, Vidal R, Piccardo P, Ghetti B, Tagliavini F, Frangione B, Prelli F: Endogenous proteolytic cleavage of normal and disease-associated isoforms of the human prion protein in neural and non-neural tissues. *Am J Pathol* 1998, 153:1561–1572
 25. Rogers M, Yehiely F, Scott M, Prusiner SB: Conversion of truncated and elongated prion proteins into the scrapie isoform in cultured cells. 1993, 90:3182–3186
 26. Bian J, Nazor KE, Angers R, Jernigan M, Seward T, Centers A, Green M, Telling GC: GFP-tagged PrP supports compromised prion replication in transgenic mice. *Biochem Biophys Res Commun* 2006, 340:894–900
 27. Notari S, Capellari S, Giese A, Westner I, Baruzzi A, Ghetti B, Gambetti P, Kretzschmar HA, Parchi P: Effects of different experimental conditions on the PrP^{Sc} core generated by protease digestion. *J Biol Chem* 2004, 279:16797–16804
 28. Cali I, Castellani R, Yuan J, Al-Shekhlee A, Cohen ML, Xiao X, Moleres FJ, Parchi P, Zou WQ, Gambetti P: Classification of sporadic Creutzfeldt-Jakob disease revisited. *Brain* 2006, 129:2266–2277
 29. Notari S, Capellari S, Langeveld J, Giese A, Strammiello R, Gambetti P, Kretzschmar HA, Parchi P: A refined method for molecular typing reveals that co-occurrence of PrP^{Sc} types in Creutzfeldt-Jakob disease is not the rule. *Lab Invest* 2007, 87:1103–1112

ORIGINAL ARTICLE

Deduction of the evaluation limit and termination timing of multi-round protein misfolding cyclic amplification from a titration curve

Atsuko Takeuchi¹, Mayumi Komiya², Tetsuyuki Kitamoto¹, and Masanori Morita²

¹Department of Neurological Science, Tohoku University Graduate School of Medicine, and ²Research and Development Division, Benesis Corporation, 2-1, Seiryō-machi, Aoba-ku, Sendai 980-8575, Japan

ABSTRACT

In this study, the efficacy of disinfectants in reducing the partially protease-resistant isoform of prion protein was evaluated by a multi-round protein misfolding cyclic amplification (PMCA) technique. Hamster brains infected with scrapie-derived strain 263K were homogenized, treated under inactivating or mock conditions, and subjected to multi-round PMCA. Four sets of serial 10-fold dilutions of mock-treated samples were analyzed. Although considerable variability was observed in the signal patterns, between the second and sixth rounds the number of the PMCA round correlated in a linear fashion with the mean dilution factor of mock-treated, infected brains, corresponding to a log reduction factor (LRF) of 3.8–7.3 log. No signals were observed in the PMCA products amplified from normal hamster brain homogenates. The mean numbers of rounds at the first appearance of the signal for 1 M and 2 M NaOH-treated samples were 4.33 and 4, respectively. Using the linear regression line as the titration curve, the LRFs of these disinfectants were found to be 6.1 and 5.8 log, respectively; these values were not significantly different. The mean number of rounds for the alkaline cleaner and sodium dodecyl sulfate were 9 and 10.33, respectively, and were outside the range of both the linear regression line and evaluation limit. The disinfectants were considered very effective because their LRFs were ≥ 7.3 log. These estimations were concordant with previous bioassay-based reports. Thus, the evaluation limit seems to be valuable in some applications of multi-round PMCA, such as disinfectant assessment and process validation.

Key words disinfectant, evaluation, prion, protein misfolding cyclic amplification.

The pathogenesis of prion disease involves conversion of a cellular isoform of the prion protein (PrP^C) into a disease-associated isoform of PrP (PrP^{Sc}) (1). In healthcare facilities, inactivation or removal of prions is a vital measure for preventing iatrogenic transmission of prion disease. Bioassay, the only method for measuring residual infectivity after inactivation, has some drawbacks. Bioassays

are expensive and time-consuming. Assessment of toxic reagents requires enormous dilution, which also reduces sensitivity. Sensitivity in animal models does not always reflect sensitivity in transmission between humans. Therefore, development of sensitive *in vitro* methods that can serve as surrogate or supplemental measures for bioassays is necessary.

Correspondence

Masanori Morita, Benesis Corporation, C/O Department of Neurological Science, Tohoku University Graduate School of Medicine, 2-1, Seiryō-machi, Aoba-ku, Sendai 980-8575, Japan.

Tel: +81 22 717 8147; fax: +81 22 717 8148; email: morita-m@med.tohoku.ac.jp

Received 15 December 2010; revised 8 February 2011; accepted 8 March 2011.

List of abbreviations: 263K-BH, brain homogenate prepared from 263K-infected hamster brain; BH, brain homogenate; CJD, Creutzfeldt-Jakob disease; LRF, log of reduction factor; N-BH, normal hamster brain homogenate prepared for PMCA substrate; NaOH, sodium hydroxide; Neg-BH, normal brain homogenate prepared for negative control; PK, proteinase K; PMCA, protein misfolding cyclic amplification; PrP, prion protein; PrP^C, cellular isoform of PrP; PrP^{Res}, partially protease resistant isoform of PrP; PrP^{Sc}, disease associated isoform of PrP; Tris, tris-hydroxymethyl-aminomethane.

Protein misfolding cyclic amplification is an *in vitro* method for producing large amounts of PrP^{res} (2). PMCA has a sensitivity >4000 times greater than that of bioassays (3), and amplified products have been shown to be infectious (4). PMCA has been used to assess the efficacy of PrP^{Sc} removal, and the reported results have been concordant with the results of bioassays to assess inactivation efficacy (5, 6). However, many bioassay-proven disinfectants have not yet been assessed by PMCA. Moreover, before this method can be applied in practice, many aspects must first be quantified; for example, the termination timing of multi-round PMCA and its quantitative capabilities.

In the present study, multi-round PMCA was applied to assess the LRFs of PrP^{res} by four agents, namely, an alkaline cleaner (mip-PC-M; Ecolab, Tokyo, Japan); 3% SDS; 1 M NaOH, (which is recommended by the World Health Organization) (7); and 2 M NaOH. The efficacy of these agents has previously been assessed by bioassays (8–10).

MATERIALS AND METHODS

Preparation of brain homogenates

A 10% (w/v) homogenate of hamster brain infected with hamster-adapted scrapie strain 263K (263K-BH) was prepared in PBS containing protease inhibitors cocktail (Roche Diagnostics, Mannheim, Germany) and sonicated with an analogue sonifier (S-250; Branson Ultrasonic, Danbury, CT, USA) for 1 min. A 10% (w/v) Neg-BH was prepared under the same conditions. Another 10% (w/v) N-BH, which was used for a PMCA substrate, was prepared by homogenization in PMCA buffer (PBS containing protease inhibitors cocktail, 1% TritonX-100, and 4 mM EDTA) followed by sonication for 1 min.

Prion inactivation procedures

263K-BH was treated with four disinfectants: an alkaline cleaner, SDS, and 1 and 2 M NaOH, as described below. Disinfectant or mock treatments of 263K-BH and disinfectant treatments of Neg-BH were performed in triplicate.

Treatment with alkaline cleaner

Ten μL of 10% 263K-BH was mixed with 90 μL of an alkaline cleaner containing 0.125 M NaOH (mip PC-M, Ecolab) and this mixture incubated for 30 min at 70°C. After incubation, the sample was neutralized to pH 7.5 with 9 μL 1 M HCl, and then 4.6 μL 1.2 M Tris-HCl (pH 8.0) was added. For a negative control, Neg-BH was treated in the same manner. For a mock treatment control,

10 μL 10% 263K-BH was mixed with 90 μL of an HCl pre-neutralized alkaline cleaner (pH 7.5) and incubated under the same conditions.

Sodium dodecylsulfate treatment

One% 263K-BH was incubated with 3.0% (w/v) SDS (total volume, 100 μL) for 5 min at 100°C and 4.6 μL 1.2 M Tris-HCl (pH 8.0) added. For a negative control, Neg-BH was treated in the same manner. For a mock treatment, 263K-BH was treated with distilled water instead of SDS.

Sodium hydroxide treatment

Sodium hydroxide treatment was performed under two conditions. Ten μL 10% of 263K-BH was mixed with 90 μL 1.1 or 2.2 M NaOH and incubated for 120 and 60 min, respectively, at 25°C. In both methods, samples were neutralized to pH 7.5 with 9 μL 10 M HCl, and 4.6 μL 1.2 M Tris-HCl (pH 8.0) was added. For a negative control, Neg-BH was treated in the same manner. A mock treatment was performed with distilled water instead of NaOH.

Multi-round protein misfolding cyclic amplification reaction

Disinfectant-treated 263K-BH (triplicate) and disinfectant-treated Neg-BH (triplicate) were diluted 1:100 in N-BH substrate, and serial 10-fold dilutions of mock-treated 263K-BH (in duplicate) were prepared by diluting with 10% N-BH substrate. The reaction mixture (total volume, 100 μL) was placed in a 0.1 mL thin-walled PCR tube with a screw cap (No. 72.733.200; Sarstedt, Numbrecht, Germany) and subjected to multi-round PMCA. A round of amplification consisted of 48 cycles of sonication (five pulses of 5sec with 1sec rest) and agitation (1 hr) at 37°C using a fully automatic cross-ultrasonic protein activating apparatus (ELESTEIN 070-GOT, Elekon Science, Chiba, Japan). After each round, the reaction products were diluted 1:10 in fresh 10% N-BH, after which the next round was started. For serially diluted mock-treated samples, multi-round PMCA was terminated when a signal was detected (with some exceptions).

Proteinase-K digestion and Western blotting

Samples were digested with PK for 30 min at 37°C; a concentration of 50 $\mu\text{g}/\text{mL}$ was used for samples before they were subjected to PMCA, and 100 $\mu\text{g}/\text{mL}$ for samples after PMCA. The digested samples were Western blotted with an anti-PrP monoclonal antibody (3F4) as described previously (11). Western blot signals were detected with a Versa Doc 5000 imaging device and signal intensities

were quantified using Quantity One software (Bio-Rad Laboratories, Hercules, CA, USA).

RESULTS

Assessment of logs of reduction factor of the partially protease resistant isoform of prion protein by four disinfectants using multi-round protein misfolding cyclic amplification

We assessed residual amounts of PrP^{res} after four inactivation procedures: alkaline cleaner treatment for 30 min at 70°C, 3% SDS treatment for 5 min at 100°C, 1 M NaOH treatment for 2 hr at 25°C, and 2 M NaOH treatment for 1 hr at 25°C. 263K-BH (1%) was treated with four inactivation procedures and neutralized. No signal was detected in undiluted, disinfectant-treated 1% 263K-BH, but strong signals were observed in 30-fold diluted, mock-treated 263K-BH (positive control) (Fig. 1a), indicating that the residual amounts of PrP^{res} were below the Western blot detection limit. To eliminate inhibition by disinfectants carried over into the PMCA reaction mixture, the disinfectant-treated 263K-BHs or Neg-BHs were diluted 100-fold in 10% N-BHs, generating 10⁻⁴ dilutions of brain, and subjected to PMCA. To evaluate the inactivation efficacy or LRF of each disinfectant individually, PMCA of serial 10-fold dilutions of relevant mock-treated samples were performed simultaneously (dilution factors used are indicated in Figs. 1b–e).

Alkaline cleaner

We detected PrP^{res} signals by Western blot in each round (Fig. 1b). Signals for two out of three alkaline cleaner-treated samples appeared in the ninth round (indicated by arrowheads in Fig. 1b). All signals for ≥ -10 log dilutions of mock-treated samples appeared by the third round, and a signal for one of the -11 log dilutions appeared in the ninth round. Thus, we inferred that the residual amount of PrP^{res} in the initial PMCA reaction mixture of alkaline cleaner-treated samples was ≤ -11 log dilution. Because there was a -4 log dilution of 263K-infected brain in the initial reaction mixture, the LRF of PrP^{res} by alkaline cleaner was calculated as ≥ 7 log.

Sodium dodecylsulfate

We detected PrP^{res} signals by Western blot in each round (Fig. 1c). Two of the SDS-treated replicates generated signals in the tenth round, and the third generated signal in the eleventh round (indicated by arrowheads in Fig. 1c). All of the ≥ -11 log dilutions generated signals by the tenth round. One -12 log replicate appeared in the fifth round and the other had not appeared by the eleventh round.

Thus, we inferred that the residual amount of PrP^{res} in the initial PMCA reaction mixture was ≤ -12 log dilution. Because there was a -4 log dilution of 263K-infected brain in the initial reaction mixture, the LRF of PrP^{res} by SDS was calculated as ≥ 8 log.

1 M or 2 M sodium hydroxide

We detected PrP^{res} signals by Western blot in each round (Fig. 1d, e). Signals for two of the 1M NaOH-treated samples were detected in the fourth round, and the signal for the third replicate was detected in the fifth round (indicated by arrowheads in Fig. 1d). In the mock-treated samples, no signal appeared for the -8 log dilutions until the fifth round. Although signals for the -12 log dilutions appeared in the fifth round, signals for one of the duplicate -10 and -11 log dilutions appeared in the fourth round, while the others appeared in the sixth round (Fig. 1d). Thus, we estimated that the residual amount of PrP^{res} in the initial PMCA reaction mixture of 1 M NaOH-treated samples was between -8 and -10 log dilutions. Because there was a -4 log dilution of 263K-infected brain in the initial reaction mixture, the LRF of PrP^{res} by 1 M NaOH was calculated to be between 4 and 6 log.

One replicate each of the 2 M NaOH-treated samples generated signals in the third, fourth, and fifth rounds (indicated by arrowheads in Fig. 1e). One each of the -8 or -9 log-diluted mock-treated samples generated signals in the second and third rounds. All of the -10 to -12 dilutions generated signals between the third and fifth rounds. One -13 log-diluted replicate generated a signal in the fifth round (Fig. 1e). Thus, we estimated that the residual amount of PrP^{res} in the initial PMCA reaction mixture of 2 M NaOH-treated samples was between -8 and -13 log dilutions. Because there was a -4 log dilution of 263K-infected brain in the initial reaction mixture, the LRF of PrP^{res} by 2 M NaOH was calculated to be between 4 and 9 log. We performed all experiments in duplicate and generated the same results on both occasions.

Titration curve of protein misfolding cyclic amplification

The rough estimates described above are due to considerable variability in the rounds at which signals for the diluted mock-treated samples appeared. Signals for samples of higher dilutions did not always appear later than did those for lower dilutions (Fig. 1b–e). We concluded that accurate assessment of the efficacy of disinfectants would require a greater number of replicate samples for each serial 10-fold dilution.

We then combined the data from the four mock treatments, which we had performed under different conditions. We first compared residual amounts of PrP^{res}

Practical use of PMCA

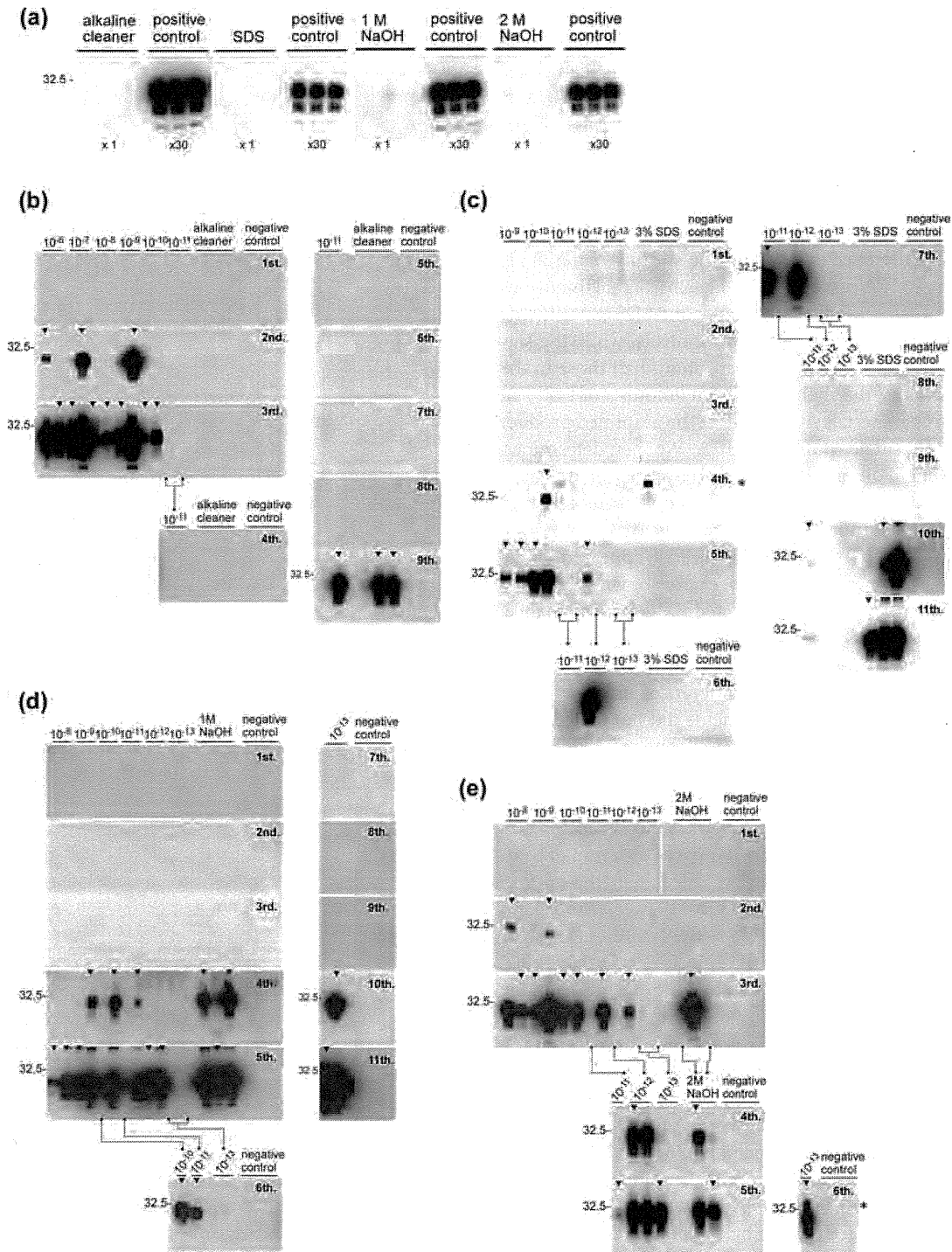


Fig. 1. Western blot analysis of PrP^{res} before and after PMCA. (a) Western blots of disinfected and mock-treated samples, containing 1% 263K-infected brain homogenate, after proteinase K digestion. Samples were undiluted ($\times 1$) or diluted 30-fold ($\times 30$) before Western blotting. The positive controls are mock-treated samples. (b–e) Western blots of PMCA products after proteinase K digestion at each round. Disinfectants include (b) an alkaline cleaner, (c) 3% SDS, (d) 1 M NaOH, and (e) 2 M NaOH. Arrowheads indicate the signal first detected from disinfected samples or from each dilution of mock-treated samples. The PMCA round number is indicated at the right top corner of each panel, and molecular mass of the protein bands (kDa) is indicated at the left of each panel. Dilution factors of mock-treated samples starting from the infected brain are provided at the top of each panel; control indicates negative control reactions. * indicates bands caused by insufficient proteinase K digestion. Connecting lines between panels indicate continuity of samples in multi-round PMCA.

between mock-treated 263K-BH before PMCA to study the direct effect of mock treatments (Fig. 2a). Signal intensities of PrP^{res} in samples treated with distilled water for 5 min at 100°C (mock treatment for SDS) were about one-fifth of those in untreated samples (controls). Signal intensities for the remaining three mock treatments were comparable to those in the controls. We then compared amounts of amplified PrP^{res} between mock-treated 263K-BH after the first round of PMCA to determine whether the slight difference in PrP^{res} in the starting material affected the PMCA product yield (Fig. 2b). Signal intensities in the mock-treated alkaline cleaner and SDS experiments were comparable to those in the controls, while the signals for 1 M and 2 M NaOH were about half those in the controls. Thus, the slightly different amounts of PrP^{res} in the starting materials did not affect the amplified product yield after a single round of PMCA. We then determined whether slight differences in amounts of PrP^{res} in the starting materials affected signal appearances during repeated PMCA rounds; rounds at which signals for 10-fold serial dilutions of four mock treatments first appeared (indicated by arrowheads in Fig. 1b–e) are shown in Fig. 3a. If the SDS mock treatment affected PMCA performance, signal appearances for SDS mock-treated samples should have been delayed. However, no remarkable delay was observed, indicating that slight differences in the amount of PrP^{res} after four mock treatments did not affect signal appearances in multi-round PMCA. Thus, we concluded that combined statistical analysis of the four sets of mock treatment data was reasonable.

To study the correlation between dilution factor and round number, the mean and standard deviation of dilution factors for each round were calculated (the bottom line of Fig. 3a) and plotted (Fig. 3b). Between the second and sixth rounds, PMCA round strongly and linearly correlated with the mean of dilution factors ($r^2=0.924$; Fig. 3b, solid line). The linear regression line extends from the -7.8 to -11.3 log dilutions. We did not observe a linear correlation after the seventh round (Fig. 3b, dashed line). Round number means for alkaline cleaner-, SDS-, 1 M NaOH-, and 2 M NaOH-treated samples were 9, 10.33, 4.33, and 4, respectively (shown as vertical lines in Fig. 3b). As the latter two are included within the linear regression range (Fig. 3b), amounts of residual PrP^{res} were estimated to be 10.1 and 9.8 log dilutions for 1 M and 2 M NaOH, respectively, using the linear regression line as a titration curve. Because there was a -4 log dilution of 263K-infected brain in the initial reaction mixture, the LRFs of PrP^{res} by 1 M and 2 M NaOH were calculated to be 6.1 and 5.8 log, respectively. These results do not appear to differ significantly, particularly in light of the large variances. As the former two are outside the range of the linear regression line, we judged that residual PrP^{res} in

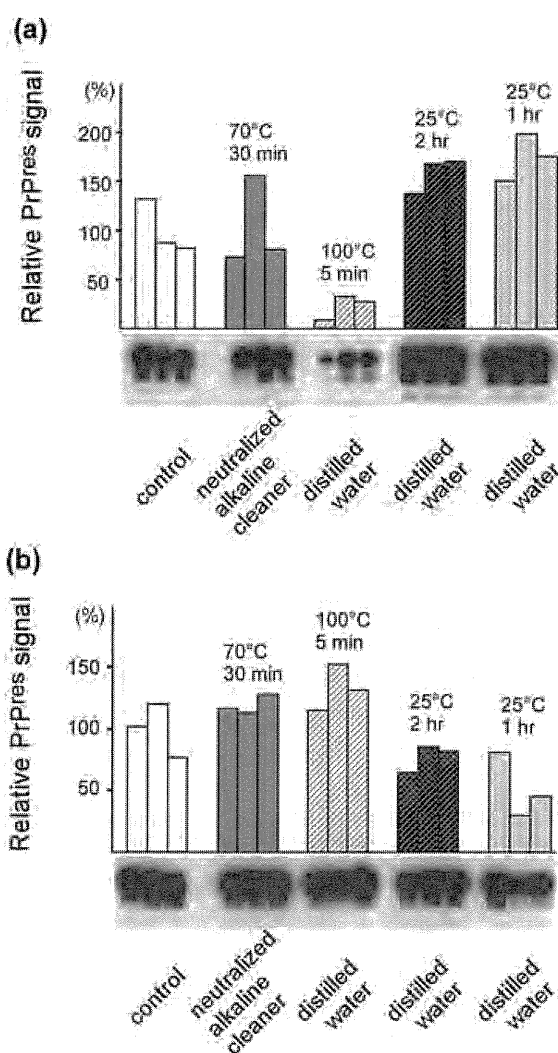


Fig. 2. The effect of mock treatments on PrP^{res} amplification by PMCA. (a) Western blot analysis of residual PrP^{res} in samples after no treatment or four different mock treatments. Physical conditions of mock treatments are indicated above the bars. The Y axis indicates relative signal intensities (percentage) versus the mean signal intensities of the controls. (b) Western blot analysis of amplified PrP^{res} after the first round of PMCA of 100-fold diluted samples shown in (a). Physical conditions of mock treatments are indicated above the bars. The Y axis indicates relative signal intensities (percentage) versus the mean signal intensities of the controls.

samples treated with alkaline cleaner or SDS are <11.3 log dilutions, which is the edge of the titration curve (Fig. 3a, bottom line). The LRFs of PrP^{res} by these disinfectants were >7.3 log.

DISCUSSION

We used multi-round PMCA to estimate minute amounts of PrP^{res} in 263K-infected hamster brain treated with four

(a)

Log ₁₀ of dilution factor	PMCA round											Signal appeared/total tested
	1	2	3	4	5	6	7	8	9	10	11	
-13					▲	▲				△	△	4/6
-12			▲	▲	●	△						5/6
-11			▲	△	▲	△	●		○	●		7/8
-10			▲	●	●	△						8/8
-9		▲	▲	△	●	●	△					8/8
-8		▲	▲	○	○	△	△					6/6
-7		○	○									2/2
-6		○	○									2/2
Mean ± SD	*	-7.8 ± 1.3	-9.1 ± 1.7	-10.4 ± 1.1	-10.3 ± 1.7	-11.3 ± 1.5	-11 †	-	-11	-12	-13	

(b)

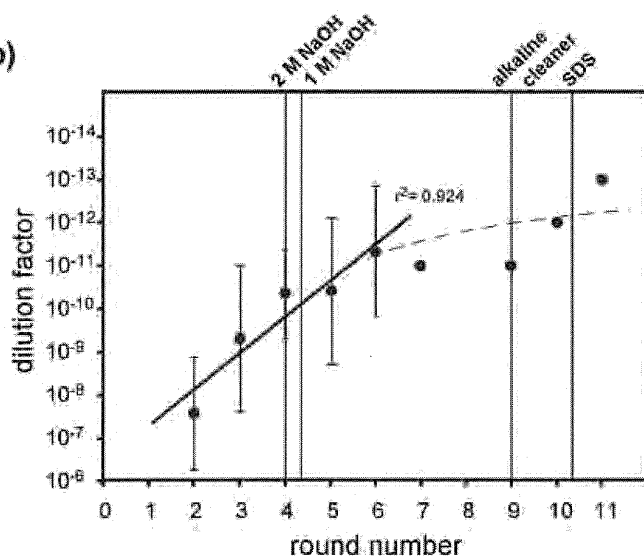


Fig. 3. Determination of the PMCA titration curve. (a) The rounds at which signals were first detected for each dilution factor of four mock treatments (indicated with arrowheads in Figs. 1b–e) are depicted. Open circles, alkaline cleaner; filled circles, 3% SDS; open triangles, 1 M NaOH; and filled triangles, 2 M NaOH. For example, in the second round of mock treatment for alkaline cleaner, one signal was detected for the 10⁻⁶, 10⁻⁷, and 10⁻⁹ log dilutions (Fig. 1b). Thus, in the row corresponding to “PMCA round” 2, one open circle is depicted on each line corresponding to “log 10 of dilution factors” of -6, -7, or -9. The mean value and SD of dilution factors of each round were calculated. *, number of PrP^{res} positive samples per total number of samples tested; †, mean and SD not calculated because no signals appeared in the first and eighth rounds; ‡, SD not calculated because the number of signals was <3 in the seventh, ninth, tenth, and eleventh rounds. (b) Filled circles and error bars indicate the mean value and SD of the dilution factors, respectively. Error bars are not shown after the seventh round because the number of signals detected was <3. Solid line, linear regression line; dashed line, fitting curve; vertical lines, means of the rounds at which signals were first detected.

disinfectants. As expected, multi-round PMCA showed higher sensitivity, we could therefore perform it more quickly than a standard bioassay. The method was sensitive enough to detect signals from -13 log-diluted samples. This sensitivity is comparable to that reported in the literature (3). As the exact nature of the seed has not yet been elucidated, the relationship between seed and infectivity, or even that between seed and PrP^{res}, is not fully understood. Therefore, we estimated the amounts of PMCA seed in samples treated with disinfectants, and calculated the LRF as the difference between the estimated amount of PMCA seed and the total PrP^{res} input in the initial PMCA reaction mixture.

The LRF of alkaline cleaner assessed by PMCA was ≥ 7.3 log (Fig. 3b). Baier *et al.* observed no infectivity in 263K-infected hamster brain homogenate treated with alkaline cleaner (12). Thus, the deduced LRFs by PMCA is consistent with assessment by bioassays. The LRF of SDS assessed by PMCA was ≥ 7.3 log (Fig. 3b). Tateishi *et al.* observed no infectivity in mouse-adapted CJD strain treated with SDS (10). As the prion strains used in PMCA and bioassay were different, direct comparison is difficult, however the tendency of the effect of SDS treatment on either strain is similar. The LRF of 1 M NaOH was 6.1 log in this study (Fig. 3b). The infectivity in 263K-infected hamster brain homogenate treated with 1 M NaOH was $< 10^{3.8}$ (calculated to be > 5.5 LRF) (15). The inactivation efficacy of 1 M NaOH on CJD Fukuoka-1 strain as determined by mouse bioassay has been reported to be 4–6 (9, 13). In one report, the authors did not observe infectivity in 263K-infected hamster brain homogenate treated with 1 M NaOH (14), but the sensitivity of the bioassay was reduced in that study because the samples were diluted to reduce NaOH toxicity. Thus, we consider that our estimation is concordant with bioassay-determined LRFs. The LRF of 2 M NaOH in this study was 5.8 log (Fig. 3b). The inactivation efficacy of 2 M NaOH assessed by bioassay is somewhat enigmatic. Mice inoculated with CJD Fukuoka-1 strain treated with 2 M NaOH developed disease after a longer incubation time than did mice inoculated with samples treated with 1 M NaOH (9). Residual infectivity in 263K-infected hamster brain homogenate treated with 2 M NaOH for 120 min was $10^{4.2}$ (calculated to be 5.1 LRF), but in samples treated with 1 M NaOH for 60 min, the residual infectivity was $\leq 10^{3.8}$ (15). Nevertheless, the LRF for 2 M NaOH estimated by PMCA appears consistent with the LRF assessed by bioassay. Collectively, the PrP^{res} LRFs for at least three procedures tested in this study were concordant with the LRFs of infectivity. These results suggest that PMCA can be used as a surrogate for, or supplement to, bioassay (5).

By analyzing the signal patterns of mock-treated samples, we found a linear correlation between PMCA rounds

and infected brain dilution factors. The linear regression line can therefore serve as a titration curve. When the mean round number of disinfectant-treated samples was inside the range of the titration curve, we could deduce the amount of PMCA seed from the curve; when it was outside the range, the estimated amount remained constant, namely ≥ 7.3 . We thus regard the edge of the titration curve as the evaluation limit. This is similar to the concept of assay system detection limits. Thus, there are two limitations of PMCA: the detection limit and the evaluation limit, which in this study were -13 log and -11.3 log dilution, respectively. Once the estimated amount of PMCA seed has become constant, we believe that continuing multi-round PMCA is fruitless. In other words, we recommend terminating multi-round PMCA after the round corresponding to the evaluation limit has been passed. The titration curve can be used in two ways: to deduce the amount of PMCA seed and to indicate the timing of termination.

The quantitative capability of the titration curve is somewhat compromised by the variability in signal appearances (Fig. 3a and b). We speculate that the reasons for this variability are as follows: (i) the efficiency of PMCA amplifications is intrinsically variable, probably due to variability in breakage of the PMCA seed by sonication, which is difficult to control (16); and (ii) dilutions prepared from aggregated material have a dilution error or lack of uniformity in PrP^{res} particle size and number. This lack of uniformity causes gain or loss of PMCA seed in highly diluted samples, which in turn biases the presence or absence of signal. To establish a quantitative PMCA analysis, further efforts are required to reduce variability. During the preparation of this manuscript, Chen *et al.* reported a linear correlation between PrP^{res} amounts and PMCA round (17). They concluded that partial purification of 263K-infected brain homogenate is important to reduce variability in PMCA.

Another objection to the use of PMCA for assessing PrP^{res} is contamination or *de novo* generation of PrP^{res}. Because PMCA is very sensitive, a trace amount of contamination yields false positive signals. We took great care to avoid contamination. Because no signal appeared in the negative controls, which do not contain 263K-BH (Fig. 1b–e), we believe that no contamination or *de novo* generation occurred in our experiments. A third objection to PMCA is the use of disinfectant. In a bioassay, animals cannot be inoculated with undiluted toxic materials. Similarly, materials that inhibit PMCA performance must be diluted, which reduces sensitivity. Hence, we diluted the SDS-treated samples.

Before PMCA can be used for assessing disinfectant efficacy, criteria by which efficacy is defined must be established. The presence or absence of signal seems to be an

inadequate criterion, because signals eventually appeared in samples treated with all four disinfectants, disinfectants that have been proved by bioassays to possess different inactivation efficacies. The noteworthy difference between very effective disinfectants (alkaline cleaner and SDS) and moderately effective disinfectants (1 M and 2 M NaOH) was the mean round numbers at which signal first appeared. The mean round numbers of the former were outside the round corresponding to the evaluation limit, while those of the latter were within the evaluation limit (Fig. 3b). The evaluation limit may be a valid means of categorizing disinfectants.

In this study, we evaluated residual amounts of PrP^{res} after treatment with bioassay-proven disinfectants and calculated the LRF of each disinfectant using multi-round PMCA. The evaluation limit, or the range within which PMCA rounds correlate with mean dilution factors of infected brain, seems to be valuable in practical applications of multi-round PMCA, such as assessment of disinfectants and process validation.

ACKNOWLEDGMENTS

This study was supported by the Program for Promotion of Fundamental Studies in Health Sciences of the National Institute of Biomedical Innovation (T.K.); a grant from the Ministry of Health, Labor and Welfare (T.K.); a Grant-in-Aid for Scientific Research from the Ministry of Education, Culture, Sports, Science and Technology (T.K.); and the Benesis Corporation and Mitsubishi Tanabe Pharmaceutical company (A.T, M.K., and M.M). We thank Prof. K. Doh-ura for kindly providing the 263K strain. M.K. and M.M. are affiliated with the Benesis Corporation, which manufactures human plasma fractionation products and where the alkaline cleaner tested in this study is used to clean pipelines. The fact that this alkaline cleaner is also used by our company had no influence whatsoever over our experimental data.

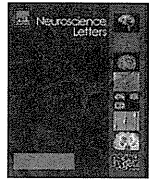
REFERENCES

1. Prusiner S.B. (1998) Prions. *Proc Natl Acad Sci U S A* **95**: 13,363–83.
2. Saborio G.P., Permanne B., Soto C. (2001) Sensitive detection of pathological prion protein by cyclic amplification of protein misfolding. *Nature* **411**: 810–3.
3. Saá P., Castilla J., Soto C. (2006) Ultra-efficient replication of infectious prions by automated protein misfolding cyclic amplification. *J Biol Chem* **281**: 35,245–52.
4. Castilla J., Saá P., Hetz C., Soto C. (2005) *In vitro* generation of infectious scrapie prions. *Cell* **121**: 195–206.
5. Murayama Y., Yoshioka M., Horii H., Takata M., Yokoyama T., Sudo T., Sato K., Shinagawa M., Mohri S. (2006) Protein misfolding cyclic amplification as a rapid test for assessment of prion inactivation. *Biochem Biophys Res Commun* **348**: 758–62.
6. Suyama K., Yoshioka M., Akagawa M., Murayama Y., Horii H., Takata M., Yokoyama T., Mohri S. (2007) Prion inactivation by the Maillard reaction. *Biochem Biophys Res Commun* **356**: 245–8.
7. World Health Organization. (2000) WHO Infection Control Guidelines for Transmissible Spongiform Encephalopathies. http://whqlibdoc.who.int/hq/2000/WHO_CDS_CSRAPH_2000_3.pdf
8. Baier M., Schwarz A., Mielke M. (2004) Activity of an alkaline 'cleaner' in the inactivation of the scrapie agent. *J Hosp Infect* **57**: 80–4.
9. Tateishi J., Tashima T., Kitamoto T. (1988) Inactivation of the Creutzfeldt-Jakob disease agent. *Ann Neurol* **24**: 466.
10. Tateishi J., Tashima T., Kitamoto T. (1991) Practical methods for chemical inactivation of Creutzfeldt-Jakob disease pathogen. *Microbiol Immunol* **35**: 163–6.
11. Ikeda S., Kobayashi A., Kitamoto T. (2008) Thr but Asn of the N-glycosylation sites of PrP is indispensable for its misfolding. *Biochem Biophys Res Commun* **369**: 1195–8.
12. Baier M., Schwarz A., Mielke M. (2004) Activity of an alkaline 'cleaner' in the inactivation of the scrapie agent. *J Hosp Infect* **57**: 80–4.
13. Tamai Y., Taguchi F., Miura S. (1988) Inactivation of the Creutzfeldt-Jakob disease agent. *Ann Neurol* **24**: 466–7.
14. Brown P., Rohwer R.G., Gajdusek D.C. (1986) Newer data on the inactivation of scrapie virus or Creutzfeldt-Jakob disease virus in brain tissue. *J Infect Dis* **153**: 1145–8.
15. Taylor D.M., Fraser H., McConnell I., Brown D.A., Brown K.L., Lamza K.A., Smith G.R. (1994) Decontamination studies with the agents of bovine spongiform encephalopathy and scrapie. *Arch Virol* **139**: 313–26.
16. Deleault N.R., Harris B.T., Rees J.R., Supattapone S. (2007) Formation of native prions from minimal components *in vitro*. *Proc Natl Acad Sci U S A* **104**: 9741–6.
17. Chen B., Morales R., Barria M.A., Soto C. (2010) Estimating prion concentration in fluids and tissues by quantitative PMCA. *Nat Methods* **7**: 519–20.



Contents lists available at ScienceDirect

Neuroscience Letters

journal homepage: www.elsevier.com/locate/neulet

Heparin enhances the cell-protein misfolding cyclic amplification efficiency of variant Creutzfeldt–Jakob disease

Takashi Yokoyama^a, Atsuko Takeuchi^b, Miyuki Yamamoto^a, Tetsuyuki Kitamoto^b,
James W. Ironside^c, Masanori Morita^{a,*}

^a Research and Development Division, Benesis Corporation, c/o Division of Neurological Science, Department of Prion Research, Tohoku University Graduate School of Medicine, 2-1, Seiryō-machi, Aoba-ku, Sendai 980-8575, Japan

^b Division of Neurological Science, Department of Prion Research, Tohoku University Graduate School of Medicine, 2-1, Seiryō-machi, Aoba-ku, Sendai 980-8575, Japan

^c National CJD Surveillance Unit, Division of Pathology, School of Molecular and Clinical Medicine, University of Edinburgh Western General Hospital, Edinburgh EH4 2XU, UK

ARTICLE INFO

Article history:

Received 23 February 2011
Received in revised form 25 April 2011
Accepted 27 April 2011

Keywords:

Heparin
Cell-PMCA
Prion
sCJD
vCJD

ABSTRACT

Highly sensitive *in vitro* screening tests are required to prevent the iatrogenic spread of variant Creutzfeldt–Jakob disease (vCJD). Protein misfolding cyclic amplification (PMCA) is a candidate for such a test, but the sensitivity of this method is insufficient. Polyanions were reported to enhance PMCA efficiency, but their effects on vCJD are unclear. We developed a cell-PMCA of vCJD, wherein cell lysate containing exogenously expressed human PrP was used as substrates, to investigate the effects of various sulfated polysaccharides on amplification efficiency. PrP^{res} amounts after cell-PMCA were analyzed by western blotting. Heparin, dermatan sulfate, and dextran sulfate (average molecular weight [MW] 1400 kDa) enhanced efficiency, but dextran sulfate (average MW 8 kDa) and a heparin pentasaccharide analog had no effect. Pentosan polysulfate inhibited cell-PMCA reaction. The amplification efficiency of cell-PMCA of vCJD increased to >100-fold per round with heparin. The enhancing effects of heparin on cell-PMCA were seed dependent: it was high for vCJD, low for sporadic Creutzfeldt–Jakob disease, and low to negligible for hamster-adapted scrapie-derived 263 K. In multi-round PMCA, signals were detected at earlier rounds with heparin than without heparin, and PrP^{Sc} in 10^{−10} diluted vCJD brain was detected by the sixth round. Heparin-assisted cell-PMCA of vCJD represents a significant step toward detecting very minute amounts of PrP^{Sc} in the body fluids of asymptomatic vCJD patients.

© 2011 Elsevier Ireland Ltd. All rights reserved.

There is growing concern that variant Creutzfeldt–Jakob disease (vCJD) may be iatrogenically transmitted from human to human [13]. For the prevention of the iatrogenic spread of vCJD, highly sensitive *in vitro* screening tests that can detect very minute amounts of the disease-associated isoform of the prion protein (PrP^{Sc}) are required. Protein misfolding cyclic amplification (PMCA) is currently one of the most sensitive methods of detecting PrP^{Sc}, because it generates large quantities of a partially protease-resistant isoform of prion protein (PrP^{res}) from materials containing PrP^{Sc} through repeated cycles of sonication and incubation [3,18,19]. PMCA was able to detect PrP^{Sc} from the brain tissue of vCJD patients [14,20]; however, human tissue was used as substrate; moreover, amplification efficiency of vCJD was considerably lower than that

of 263 K, scrapie-derived hamster-adapted strain. Various additives enhance PMCA or *in vitro* conversion efficiency of animal prion diseases [16,21,22]. However, the effect of polyanions on PMCA depends on prion strains [6], and the effect is ill defined for vCJD. In this study, we developed cell-PMCA [4] of vCJD, because cell lysate used as substrate is inexpensive, readily available, and free from ethical matters, and studied whether various sulfated polysaccharides were able to increase the PMCA efficiency of vCJD.

Human brain tissue of a vCJD patient (No. 96-07) was obtained from the brain bank of the UK National CJD Surveillance Unit. Human brain tissue from a sporadic Creutzfeldt–Jakob disease (sCJD) patient (H3) was obtained at autopsy after informed consent was received for its use for research purposes [15]. Golden hamster brain infected with 263 K was kindly gifted by Prof. Doh-ura (Tohoku University). This study was performed with the approval of the local committee on ethics.

Low-molecular-weight (LMW) heparin sodium salt, with an average molecular weight (MW) of 4–6 kDa, was purchased from LKT Laboratories (Paul, MN, USA). High-molecular-weight (HMW) heparin sodium salt, with an average MW of 13–17 kDa, was from EMD Chemicals (Gibbstown, NJ, USA). Fondaparinux sodium was

Abbreviations: BSE, bovine spongiform encephalopathy; HMW, high molecular weight; LMW, low molecular weight; MW, molecular weight; PMCA, protein misfolding cyclic amplification; PPS, pentosan polysulfate; PrP, prion protein; sCJD, sporadic Creutzfeldt–Jakob disease; vCJD, variant Creutzfeldt–Jakob disease.

* Corresponding author. Tel.: +81 22 717 8147; fax: +81 22 717 8148.

E-mail address: morita-m@med.tohoku.ac.jp (M. Morita).

0304-3940/\$ – see front matter © 2011 Elsevier Ireland Ltd. All rights reserved.
doi:10.1016/j.neulet.2011.04.072

from GlaxoSmithKline (Tokyo, Japan). Dermatan sulfate 1 sodium salt, dextran sulfate sodium salt, with average MW of 1400 kDa and dextran sulfate sodium salt, with average MW of 8 kDa were from MP Biomedicals (Solon, OH, USA). PPS was kindly gifted by Prof. Doh-ura (Tohoku University) [7]. Each polysaccharide, except Fondaparinux, was dissolved in water to a final concentration of 100 mg ml⁻¹ and stored at 4 °C.

Human brain tissue derived from the sCJD or vCJD patients and golden hamster brain infected with 263 K were homogenized in 9 volumes (w/v) of homogenization buffer A (phosphate buffered saline containing protease inhibitors cocktail [Roche Diagnostics, Tokyo, Japan]). cDNAs for chimeric PrP between mouse and human, with methionine at codon 129 (129M), or between mouse and golden hamster were constructed as described previously [11]. Amino acid sequences encoded by these cDNAs are identical to human or hamster PrP except for the N-terminal signal sequences, which are derived from mouse PrP. cDNAs were subcloned into pIRESneo3 (Takara, Kyoto, Japan). Transient expression of hamster PrP was carried out as follows: 1.6 mg of polyethylenimine "Max" (nominally MW 40,000; Polysciences Inc., Warrington, PA, USA) was dissolved in 25 ml of Opti-MEM I (Invitrogen™, Life Technologies Corp., Carlsbad, CA, USA) and incubated at room temperature for 10 min. Thereafter, 0.4 mg of expression vector for hamster PrP was dissolved in 2 ml of Opti-MEM I, mixed with polyethylenimine solution, incubated at room temperature for 10 min, and transferred into a culture flask containing 4 × 10⁸ FreeStyle 293F cells (Invitrogen™). The cells were collected 72 h after transfection, washed twice in phosphate buffered saline, resuspended in 4 volumes of PMCA buffer A (to a final concentration of 50 mM 4-(2-hydroxyethyl)-1-piperazineethanesulfonic acid [pH 7.6], 80 mM NaCl, 4 mM ethylenediaminetetraacetic acid, and 1% NP-40 [Calbiochem™]), and sonicated using Sonifier 250 (Branson Japan, Tokyo, Japan). To prepare cells that stably expressed human PrP, FreeStyle 293F cells were first adapted to adherent culture by adding 10% (v/v) fetal bovine serum (Invitrogen™) to Dulbecco's modified Eagle medium GlutaMAX (Invitrogen™). The cells were then transfected with the expression vector for human PrP with Lipofectamine 2000 (Invitrogen™), according to the manufacturer's instruction. On the day after the transfection, the cells were suspended with trypsin, spread onto 96-well plates

at a concentration of less than 40 cells per well, and cultured with 200 µg ml⁻¹ geneticin (Invitrogen™). Cells expressing the highest levels of human PrP were selected by western blot analysis, adapted to suspension culture, and maintained in FreeStyle expression medium supplemented with geneticin. Cell lysates were prepared as described above. Human and hamster PrP^C concentrations in 20% (w/v) cell lysates were greater than the hamster PrP^C concentration in 10% hamster brain homogenate (Fig. S1). Normal hamster brain was homogenized in 4 volumes of 2× PMCA buffer B (2× phosphate buffered saline, 8 mM ethylenediaminetetraacetic acid, 2% Triton X-100, and 2× protease inhibitors cocktail) and diluted by half with water just before use. Cell lysates or brain homogenates were stored at -80 °C in small aliquots.

The vCJD brain homogenate, 263 K-infected brain homogenate, and substrates were thawed, briefly centrifuged, mixed, placed in a 100 µl thin-walled PCR tube with a rod and a screw cap (Sarstedt, Numbrecht, Germany), and subjected to PMCA (in a total volume of 100 µl). sCJD brain homogenate was similarly prepared except that centrifugation was omitted. Sulfated polysaccharides were added at the indicated concentrations. One round of PMCA consisted of 48 cycles of sonication (5 sets of 5-s pulses at 1-s intervals; a power selector was set at "strong") and incubation (37 °C for 1 h). PMCA was performed with a fully automatic cross-ultrasonic protein-activating apparatus (ELESTEIN 070-GOT; Elekon Science Corp., Chiba, Japan). During PMCA, samples were continuously rotated at 2 rpm. For multi-round PMCA, PMCA products were diluted 1:3 in fresh substrate before the next round of PMCA.

Before and after PMCA samples were digested with 50 µg ml⁻¹ proteinase K at 37 °C for 60 min. The samples were then subjected to western blotting as previously described [12] with the following modifications: the primary and secondary antibodies were diluted in wash buffer (25 mM Tris-HCl [pH 8.25], 150 mM NaCl, 0.1% Tween 20) and 0.5% (w/v) skimmed milk, and the membranes were washed in wash buffer.

Cell-PMCA was performed to investigate the effects of various sulfated polysaccharides on amplification efficiency of vCJD. We amplified 10⁻⁴ dilution of vCJD brain and compared signal intensities of PrP^{res} after PMCA with and without additives by western blotting (Fig. 1A–E). PrP^{res} amounts after amplification sometimes varied considerably (for example, see "no additives" in Fig. 1E). The

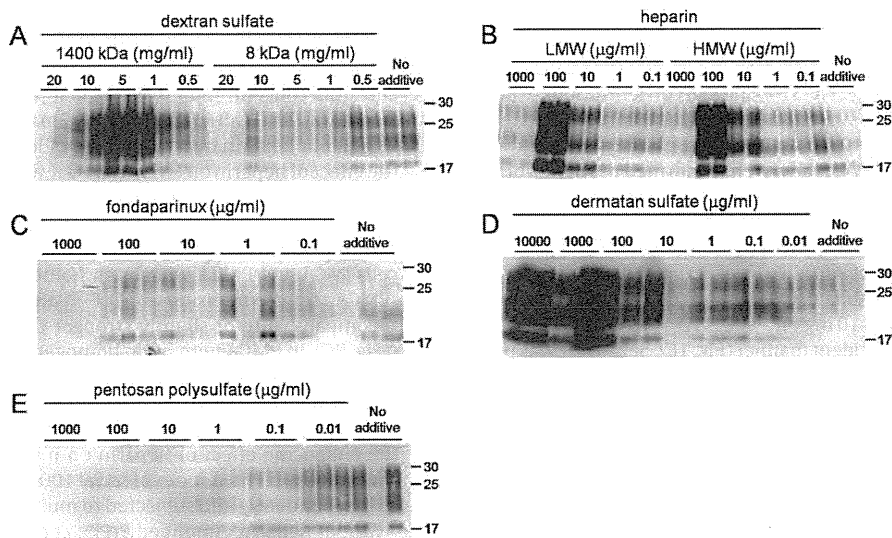


Fig. 1. Western blotting of cell-PMCA products with and without additives. Western blotting of PMCA products with and without various concentrations of sulfated polysaccharides (A–E) is shown. Molecular weight at the top of panel A indicates the mean molecular weight of dextran sulfate. LMW indicates low molecular weight. HMW indicates high molecular weight. No additive indicates that PMCA was performed without sulfated polysaccharides. Positions of molecular weight markers in kDa are indicated at the right of each panel.